NUMERICAL ANALYSIS OF BLAST PRESSURE PARAMETERS ON HUMAN WITH AND WITHOUT WALL AS A BARRIER

NURUL AINA BINTI MARUDIN

B. ENG (HONS.) CIVIL ENGINEERING

UNIVERSITI MALAYSIA PAHANG

UNIVERSITI MALAYSIA PAHANG

DECLARATION OF THESIS AND COPYRIGHT

Author's Full Name	:	NURUL AINA BINTI MARUDIN
Date of Birth	:	05 JANUARY 1996
Title	:	NUMERICAL ANALYSIS OF BLAST PRESSURE PARAMETERS ON HUMAN WITH AND WITHOUT WALL AS A BARRIER
Academic Session	:	2018/2019

I declare that this thesis is classified as:

☐ CONFIDENTIAL	(Contains confidential information under the Official Secret Act 1997)*
☐ RESTRICTED	(Contains restricted information as specified by the organization where research was done)*
☐ OPEN ACCESS	I agree that my thesis to be published as online open access (Full Text)

I acknowledge that Universiti Malaysia Pahang reserves the following rights:

1. The Thesis is the Property of Universiti Malaysia Pahang
2. The Library of Universiti Malaysia Pahang has the right to make copies of the thesis for the purpose of research only.
3. The Library has the right to make copies of the thesis for academic exchange.

Certified by:

(Student's Signature)	(Supervisor's Signature)
Nurul Aina Binti Marudin	Dr. Mazlan Bin Abu Seman
New IC: 960105-10-6214	Name of Supervisor
Date: 17/06/2019	Date: 17/06/2019

NOTE : * If the thesis is CONFIDENTIAL or RESTRICTED, please attach a thesis declaration letter.

STUDENT'S DECLARATION

I hereby declare that the work in this thesis is based on my original work except for quotations and citations which have been duly acknowledged. I also declare that it has not been previously or concurrently submitted for any other degree at Universiti Malaysia Pahang or any other institutions.

(Student's Signature)

Full Name : NURUL AINA BINTI MARUDIN

ID Number : AA15173

Date : JUNE 2019

NUMERICAL ANALYSIS OF BLAST PRESSURE PARAMETERS ON HUMAN WITH AND WITHOUT WALL AS A BARRIER

NURUL AINA BINTI MARUDIN

Thesis submitted in fulfillment of the requirements
for the award of the
B. Eng (Hons.) Civil Engineering

Faculty of Civil Engineering and Earth Resources

UNIVERSITI MALAYSIA PAHANG

JUNE 2019

ACKNOWLEDGEMENTS

I am grateful and would like to take this opportunity to express my gratitude to those who helped me during the process of completing my final year project especially my supervisor Dr Mazlan Abu Seman. I am appreciated her germinal ideas, professional advices, invaluable as well as continuous guidance, encouragements, constant support and motivation in making this research possible. He is always impressed me with his outstanding and professional conduct with his strong conviction for engineering science. I am appreciated his consistent support and effort from the first day I applied to conduct my graduate program under his supervision to these concluding moments. I am truly grateful for his progressive vision about my research in science, tolerance of my careless mistakes, and his commitment to my research study.

My sincere thanks also to all my friends and research partners who have been helping me in many ways and made my stay at UMP pleasant and unforgettable. I would like to acknowledge their comments and suggestions which are vital for the successful completion of this research study. Besides that, I am here to specially thanks to the staff of Design Laboratory who always give corporation to allow me to use the facilities in the computer laboratory.

Last but not least, I am appreciated with my sincere indebtedness and gratitude to my family for their loves, supports, motivations, and sacrifice throughout my life especially my parents who always encouraged me to accomplish my goals no matter I was up and down. I am deeply indebted to everyone who has been helping me throughout my study. Thank you.

ABSTRAK

Letupan adalah tekanan ke atas dan lebih daripada tekanan atmosfera biasa yang disebabkan oleh gelombang kejutan. Dalam era hari ini, mengkaji kesan beban letupan ke atas manusia telah menjadi penting kerana terdapat peningkatan dalam kes kecederaan manusia dan kematian yang disebabkan oleh kejadian letupan. Tekanan letupan akan menjejaskan kawasan sekitarnya yang pastinya menyebabkan kecederaan dan kematian. Dinding sebagai benteng boleh dibina sebagai salah satu pendekatan yang berkesan untuk memastikan keselamatan manusia dari kejadian letupan. Penyelidikan lanjut mengenai kesan letupan ke atas benteng diperlukan untuk memberikan idea reka bentuk struktur yang ideal. Dalam tesis ini, matlamat kajiannya adalah untuk menyiasat tekanan letupan sebanyak 13.61kg yang bersamaan dengan 30 lbs. Trinitrotoluene (TNT) ke atas dinding dan sekitarnya dan juga untuk mengkaji kesan tekanan letupan pada manusia dengan dinding dan tanpa dinding sebagai penghalang. Kajian ini memberi tumpuan kepada analisis numerik antara dua kes yang terlibat sebagai situasi kajian; kes (1) analisis numerik parameter tekanan letupan keatas manusia tanpa dinding, dan kes (2) analisis numerik parameter tekanan letupan keatas manusia dengan dinding sebagai penghalang. Parameter letupan yang diperolehi daripada keputusan numerik dibandingkan dengan ujian letupan dimana perisian AUTODYN bukan sejajar. Ia digunakan untuk membina model struktur yang disahkan melalui keputusan unjian yang diterbitkan seperti data tekanan letupan yang direkodkan pada kajian yang terdahulu. Kajian ini menilai tekanan letupan yang dihasilkan oleh beban letupan sebanyak 30lbs. TNT pada manusia di beberapa lokasi. Oleh itu, hasil penyelidikan untuk kajian ini adalah untuk menentukan kesan tekanan letupan pada manusia sama ada akan menyebabkan sebarang kecederaan atau kematian. Pengetahuan tentang tekanan letupan yang diramalkan secara numerik dalam makalah ini diterima untuk pemahaman terperinci. Keputusan numerik yang diperolehi pada kedudukan lokasi yang berbeza dibentangkan dan dibandingkan. Hasil analisis menunjukkan bahawa tekanan letupan berkurangan apabila terdapat dinding sebagai penghalang berbanding dengan ketika tiada kehadiran dinding. Selain itu, keputusan seperti yang ditunjukkan dalam graf tekanan-masa menunjukkan bahawa tekanan letupan bertindak dalam penurunan nilai dengan masa dan jarak yang semakin meningkat. Seperti dalam analisis numerik, nilai tertinggi yang terhasil dalam parameter tekanan letupan dalam kawasan lapang (kes 1) ialah 690 kPa yang memberi impak terdedah kepada 100% kemungkinan kematian dan kecederaannya adalah dari gegendang telinga pecah dan paru-paru rosak. 125 kPa pada kes 1 adalah nilai pada puncak terendah dimana keputusannya ialah kebanyakan orang terbunuh dan kemungkinan kecederaan adalah 50% pecah gegendang telinga dan kemungkinan paru-paru rosak. Manakala dalam kes 2 pula puncak tertinggi bernilai 256 kPa yang mempunyai kesan berdasarkan kajian literatur disimpulkan sebagai sedikit kemungkinan kerosakan paru-paru, kemungkinan gegendang telinga pecah, dan hampir 100% kematian. Untuk puncak minimum dalam kes 2 iaitu 125 kPa, ia mendapat kesan ke atas manusia yang sama dengan kesan puncak minimum kes 1. Keputusan yang diperoleh daripada kajian ini boleh digunakan untuk membantu kajian masa depan mengenai tekanan letupan pada manusia.

ABSTRACT

Blast is the pressure over and above normal atmospheric pressure caused by a shock wave. In today's era, studying the impact of blast load on human has become important due to the increase in cases of human injury and fatality caused by events of explosion. The blast pressure will affect the surrounding area will definitely cause human injury and fatality. Barrier walls can be built as one of the effective approaches from possible explosion events to ensure human safety. Further investigation on the impact of blast load on the barrier is needed to provide an ideal structural design as the barrier. In this thesis, the aim of this study is to investigate blast overpressure of 13.61kg which is equivalent to 30 lbs. Trinitrotoluene (TNT) to a wall and its surrounding and to study the effect on blast pressure subjected to human with and without wall as a barrier. This study is focusing on the numerical analysis between two cases involved as possible situations which are; Case 1- numerical analysis of blast pressure parameters on human without wall, and Case 2- numerical analysis of blast pressure parameters on human with wall as a barrier. The acquired blast parameters from numerical results are compared with blast test where AUTODYN non-linear finite element (FE) analysis commercial software is used to develop a validated numerical model against published experimental result such as recorded blast pressure data. This research appraises the possible blast pressure produced by blast load of 30lbs TNT on human at selected location. Thus, research outcome for this study is to determine the effect of blast pressure on human will cause any casualty or fatality. The existing knowledge of predicted blast pressure numerically has been embraced in this paper for detail understanding. The numerical result obtained at different position on the structure are also presented and compared. The result analysis shows that blast pressure is reduced when there is a wall as barrier compared to when there is no presence of wall. In addition, the result as presented in pressure-time graph shows that blast pressure behaves in decreasing manner against increasing time and distance. As in the numerical analysis, it resulted with the highest peak in blast pressure parameter in free field (Case 1) is 690 kPa which the impact on human is prone to possible 100% fatality approach and the injury is from rupture eardrum and damaged lungs. While the minimum peak pressure in Case 1 is 125 kPa which have the effect of possible most people are killed and the possible injury is 50% chance of eardrum rupture and possible damaged lungs. Whereas the highest peak pressure in case 2 is 256 kPa which has the effects based on literature review concluded as slight chance of severe lung damage, possible rupture eardrum, and approach 100% fatalities. For the minimum peak of 125 kPa in case 2 is resulted with similar effect to minimum peak pressure in case 1. The results obtained from this study can be used to assist in future study on blast pressure parameters on human.

TABLE OF CONTENT

DECLARATION

TITLE PAGE

ACKNOWLEDGEMENTS ii

ABSTRAK iii

ABSTRACT iv

TABLE OF CONTENT v

LIST OF TABLES vii

LIST OF FIGURES viii

CHAPTER 1 INTRODUCTION 1

1.1 Research Background 1

1.2 Problem Statement 1

1.3 Objectives of The Research 1

1.4 Scope of The Research 1

1.5 Significant of The Research 2

1.6 Outline of The Thesis 3

CHAPTER 2 LITERATURE REVIEW 4

2.1 Introduction 4

2.2 Blast 4

2.2.1 Blast Loading Classification 7

2.2.2 Propagation of The Blast Wave 8

2.2.3 Blast Impact on Human 3

2.3 AUTODYN 6

2.3.1 Material Model for Concrete 7

2.3.2 Material Model for Steel Reinforcement 10

2.3.3 Material Model for Air and High Explosive 11

2.4 Summary 11

CHAPTER 3 METHODOLOGY 13

3.1 Introduction 13

3.2 Numerical Modelling in AUTODYN 14

3.2.1 Blast Pressure Analysis 20

3.3 Summary 22

CHAPTER 4 RESULTS AND DISCUSSION 23

4.1 Introduction 23

4.2 Numerical Analysis of 30 lbs. TNT 23

4.3 Blast Pressure Analysis 24

4.3.1 Blast Pressure Parameter for Case 1 24

4.3.2 Blast Pressure Parameter for Case 2 25

4.4 Blast Pressure Effect on Human 27

4.5 Summary 30

CHAPTER 5 CONCLUSIONS AND RECOMMENDATIONS 31

5.1 Conclusions 31

5.2 Recommendations 32

REFERENCES 33

LIST OF TABLES

Table 2.1 Wave form constant β in relation to scaled distance Z 6

Table 2.2 Categories of Blast Load 7

Table 2.3 Improvised Explosive Device (IED) safe stand-off distance 13

Table 2.4 Bomb threat evacuation and its recommended distances 1

Table 2.5 Blast pressure effect on unprotected human 5

Table 2.6 Human ear damage due to blast pressure. 5

Table 2.7 Human lung damage due to blast pressure. 6

Table 2.8 Effect of increasing blast pressure on human 6

Table 3.1 Employed material data for Concrete input to the RHT 15

Table 3.2 Employed material data for TNT, input to the JWL EOS 17

Table 3.3 Employed material data for air, input to the ideal gas EOS 19

Table 3.4 Employed material data for TNT, input to the JWL EOS 19

Table 4.1 Maximum Peak of Blast Pressure 23

Table 4.2 Results of peak pressure without RC wall as a barrier 24

Table 4.3 Results of peak pressure with RC wall as a barrier 25

Table 4.4 Pressure difference in Case 1 and Case 2 27

Table 4.5 Blast pressure effect on human in Case 1 28

Table 4.6 Blast pressure effect on human in Case 2 29

LIST OF FIGURES

Figure 2.1 Illustration of Blast Wave Propagation 5
Figure 2.2 Typical ideal free-air blast wave pressure-time graph 5
Figure 2.3 Classical ground reflection 6
Figure 2.4 Blast wave from a surface burst 9
Figure 2.5 Illustration of Friedlander curve with maximum effective radius of primary and secondary blast injuries of an open spaced without any barrier wall, 155 mm mortar shell explosion with 200 lbs (100 kg) of TNT equivalent 10
Figure 2.6 Position of human body. (a)No obstruction of incident wave: $P=P_s$. (b)Diffraction of incident wave: $P=P_s$+Q. (c)Body subjected to reflection (standing): $P=P_r$, (d) Body subjected to reflection (prone): $P=P_r$ 11
Figure 2.7 Chart of blast pressure against stand-off distance 12
Figure 2.8 Blast wave diffraction over a barrier wall. 2
Figure 2.9 Illustration of primary, secondary, and tertiary blast injury 4
Figure 2.10 Maximum strength, yield strength and residual strength surfaces. 8
Figure 2.11 Third invariant depend on stress π plane. 9
Figure 3.1 Methodology Flow Chart 13
Figure 3.2 ALE solver technique in AUTODYN 14
Figure 3.3 Eight nodes hexahedral element. 14
Figure 3.4 The 1 m wedge (2D) filled with TNT and air. 18
Figure 3.5 Pressure contours in 1 m wedge (3D) during solving progress. 18
Figure 3.6 blast pressure at 18 ft from centre of charge weight. 20
Figure 3.7 Pressure gauge plotted in case 1. 21
Figure 3.8 Pressure gauges plotted in Case 2. 21
Figure 3.9 Blast simulation flow with RC wall as a barrier. 22
Figure 4.1 Peak blast pressure between numerical simulation and actual blast test. 24
Figure 4.2 Pressure profile without RC wall 25
Figure 4.3 Pressure profile with RC wall 26

CHAPTER 1

INTRODUCTION

1.1 Research Background

Nowadays terrorist attack at attraction place are easily can be heard or reported in news. The purpose of this terrorist attack to attract attention from the authority or demand something in return from their act. According to the Department of Army, the most favourable method is using explosive threat such as Improvised Explosive Device (IED). This act caused blast pressure ejected to the surrounding area and damage anything in its path. Part of the damage cause are human injury and fatality. Besides the explosive materials mentioned, the accidental accident such as transformer, factory plant, gas pipeline and vehicle explosion are also the possible source to generate blast pressure to the surrounding (Kabu et al., 2015).

Reinforced concrete walls (RC wall) as barrier can be built as one of the effective approaches from possible explosion events to ensure human safety (Rouse and Consultants, 2012). To provide an idea of blast pressure on human, a study of blast load impact with and without the barrier is needed. Consequently, the after effect of the blast pressure must be identified in order to determine the strength and impact blast load on the barrier at specific parameters. The data obtained will then be evaluated to determine whether the pressure value and the trends in the data chart will either increase or decrease under different conditions. Based on the data analysis, the results are then compared and discussed to determine the structure's viability at specific blast pressure to ensure that human safety is maintained.

1.2 Problem Statement

Lethal injury on human due to blast explosion is the mostly reported. The higher the amount of the explosive, the higher percentage for the fatal will be. As reported in the newspaper of Berita Harian, the explosion occurred at flat housing unit in Sibu that had caused eleven people injured and some victims reported burned (Kawi, 2015). Such an incident has made the public aware of the practice of safety and to be more cautious against sources that can cause an explosion, as it has been shown that blasting can affect human beings with such injury and fatality. The news shows such explosion events does not guarantee safety of the civilian. Besides, most civilian infrastructures are not design to withstand the blast load pressure and thus will cause death to people on the surrounding area. As a consequence, this research will help in determining the suitable implementation for safety purposes because the present work aim to understand the blast pressure effect on human depending on parameters affecting blast impact such as presence of wall as protection barrier, standoff distance.

1.3 Objectives of The Research

The following are the objectives of this research:

1. To investigate blast overpressure of 13.61 kg (30 lbs) Trinitrotoluene (TNT).
2. To study the effect of blast pressure on human with and without wall as a barrier.

1.4 Scope of The Research

To fulfil the research objective, this research aim to study about the blast pressure behaviour is to determine the extent of the 30 lbs capability of the explosion to give impact towards its surrounding and to study on the blast pressure subjected to human with and without wall as a barrier. In order to established the mentioned objectives of the present research, the scope research can be explained as follows:

1. The 30 lbs. blast is modelled numerically in AUTODYN 3D non-linear finite element (FE). Then the simulation is verified by blast overpressure available in a literature by (Yan et al., 2016). It considers the similarities in numerical analysis results and experimental results. The parameters involved as similar fixed variables between the numerical simulation and the experimental analysis are

such as distance of explosion from object, height of pressure transducer, types of explosion, and blast weight.

2. This research consists of two case studies which are; Case1 blast pressure without wall as a barrier, and Case 2 blast pressure with wall as a barrier. This research involved the volume of air modelling and the structural modelling together with its details. Case 1 indicates an open space condition where blast is directly impacted to the transducer while Case 2 represents a condition of a wall existence as a barrier to the blast event. Then these two cases are analysed in the ANSYS AUTODYN numerically. The simulation is conducted to gain better understanding about the blast where the data obtained from the numerical simulation is discussed and evaluated.

3. This research will also cover on the possible impact on human due to the blast load. At different conditions such in Case 1 and Case 2, the relationship of blast load pressure and its impact on human is determined whether it caused casualty and fatality or not at a specific blast pressure amount. Moreover, the result is discussed and evaluate based on the literature review of blast pressure impact on human such as from journal, website, books, and any other sources related to blast effect.

1.5 Significant of The Research

Firstly, this research study provides a 3-dimensional (3D) numerical model of blast. A 30 lbs TNT blast is modelled and then verified before it is applied to case studies. Since the application of modelling and numerical analysis is done in 3D, hence it is pertinent to be used as reference to the real-world implementations. This research study also is a significant endeavour in interpreting and analysing blast load behaviour. It provides more information for future research subjected to blast pressure. Since this research validated numerical modelling vs experimental analysis, therefore study is possible to carry out as there is limited access for civilian to conduct actual blast test. Furthermore, this research is helpful and beneficial to the construction industry and business practitioners since most civilian infrastructures are not design to withstand the blast pressure. These parties can implement it to a new invention or practice in their training and in the developed and construction management area. Considering blast load pressure to a structure and its surrounding will be useful in terms of taking precautionary measures against the disaster and unexpected events involving explosion. Other than that, with this research study on blast load effects, possible damage such as damages on infrastructure, injury on human, and fatality can be predicted. This is due to the significant understanding of the pressure parameters numerically and having the literature review comparison provides more information on the blast pressure behaviour on different conditions.

1.6 Outline of The Thesis

Chapter 1 presents aa general introduction and a discussion of the problem, the objectives, and the scope of the research as well as significance of the research.

Chapter 2 contains two topics covered by this research, namely the blast overview and its context, and the numerical investigation of the blast parameters using AUTODYN.

Chapter 3 describes the methodology to investigate the blast parameters with and without wall numerically.

Chapter 4 presents the numerical modelling of blast pressure according to the literature and analysis of the blast pressure with and without wall. The results are established and are considered for subsequent analysis in the present research.

Chapter 5 discussed about the conclusion of the overall thesis. This chapter concludes the contents of this present thesis from chapter 1 to chapter 4. Then, recommendations from the overall conclusion is also included in this chapter where several suggestions to improvise the data and findings in the present study is stated at the end of this thesis.

CHAPTER 2

LITERATURE REVIEW

2.1 Introduction

The purpose of literature review was to study the theoretical background of blast pressure parameters on human with and without wall as a barrier through journals, books, internet, and articles. This chapter presents two topics covered by this research, namely the blast overview and its context, and the numerical investigation of the blast parameters using AUTODYN. The blast overview includes blast load classification, propagation of the blast and its reflection, and blast impact on human. The section of numerical simulation using AUTODYN covers the material model for concrete, steel reinforcement, air and high explosive.

2.2 Blast

There are ways to blast happen which will differential the working of severity to effect on any construct structure. So, what happen is every blast will generate blast wave that will propagate from blast point to nearby structures as shown in Figure 2.1, the reflection from the ground in the air collide through the structure in a phase of wave front.

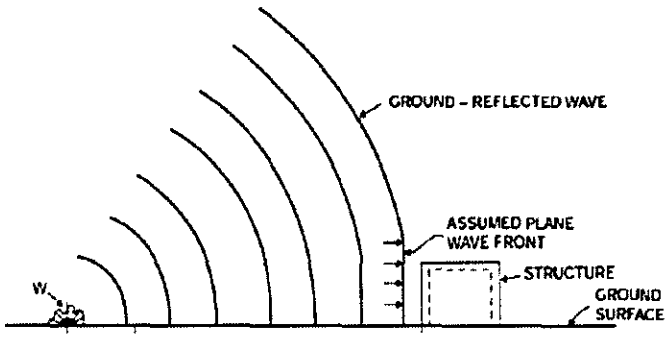

Figure 2.1 Illustration of Blast Wave Propagation

Source: Kerampran et al. (2016)

When this explosive effect is obtained from the propagation of the blast wave structure, the general blast wave pressure-time history is found as shown in Figure 2.2. Key blast wave parameters associated with ideal blast waves include peak positive overpressure, peak negative under pressure, dynamic pressure, positive and negative phase duration, and positive and negative phase impulses, integral to the time of the respective pressures.

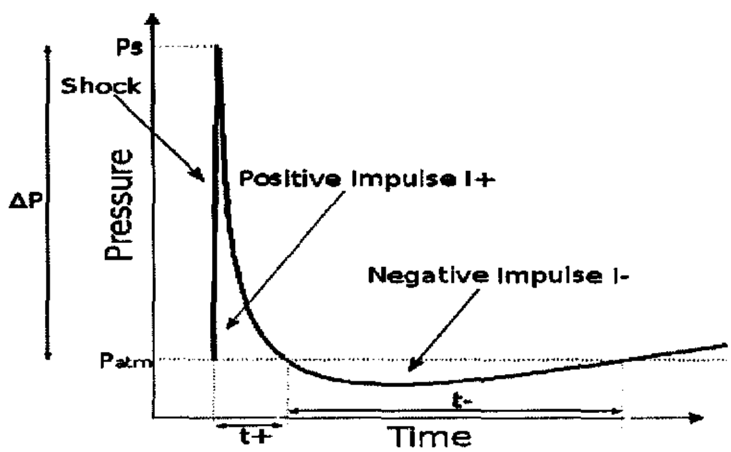

Figure 2.2 Typical ideal free-air blast wave pressure-time graph

Source: Kerampran et al. (2016)

According to (Kerampran et al., 2016), P_{so}, a peak positive blast pressure, is a pressure over the value of ambient pressure P_o, P_{so}^{-}, a negative under pressure, is a pressure below the ambient pressure. Dynamic pressure $q_o^{'}$ is the pressure formed by the movement of gas particles behind the moving shock front. Dynamic pressure magnitude, particle velocity, and air density are a function of peak incident pressure. The positive phase of a blast wave in Figure 2.2 is described by Friedlander formula:

$$P_s(t) = P_s \times \left(1 - \frac{t-t_A}{t_o}\right) \times exp\left(-\beta \frac{t-t_A}{t_o}\right) \quad (1)$$

where t_A is the arrival time, t_o is the positive phase duration, and β is wave form constant depending on the shape of the wave front as shown in Table 2.1.

Table 2.1 Wave form constant β in relation to scaled distance Z

Z (m/kg$^{1/3}$)	β (-)
0.4	8.50
50	0.5

Source: Kerampran et al. (2016)

Before being strengthened, free air bursts occur when the wave reaches the structure. If the wave reaches the ground before reaching the structure, its reflection from the ground may need to be taken into account. There are two types of reflections can occur: classical as shown in Figure 2.3 or reinforcement reflection as shown in Figure 2.1. This phenomenon depends on the angle of incidence between ground and incident wave where 40° is assumed as a critical angle. The resulting incident and reflected wave magnitude are higher and the relationship between pressure and time is modified. Surface air bursts occur when the detonation of the load occurs on or near the ground. In such a case, incident and reflected waves are merged close to the point of detonation.

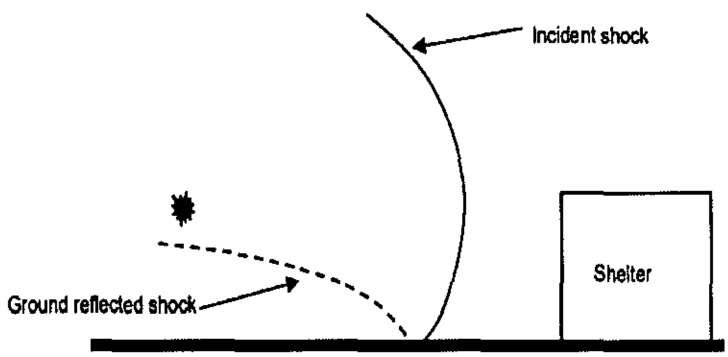

Figure 2.3 Classical ground reflection

Source: Mamrak et al. (2011)

Three main effects on the structure caused by a blast load: blast pressures, fragments generated by explosion, and shock loads produced by the shock wave and transmitted through the air or ground. The latter are loads that produce transient vibrations of soil and structure. Various methods of estimating the blast peak pressure were based on a scaled distance, which is denoted as:

$$Z = \frac{R}{W^{\frac{1}{3}}} \qquad \left[\frac{m}{kg^{\frac{1}{3}}}, \frac{ft}{lb^{\frac{1}{3}}}\right] \tag{2}$$

Where R is the distance to the charge, and W is the charge's mass.

Depending on where they are located, explosive, internal and external explosions can be identified. Subsequently, only external explosion is discussed, but there is no big difference between these two types except that blast wave-structure interactions are even more complex and multiple reflections occur in the case of internal explosions. External air blasts can be divided into free air bursts, air bursts and bursts of surface air.

2.2.1 Blast Loading Classification

Blast loads can be classified into two major groups that are explosions unconfined and confined based on the explosive load as shown in Table 2.2. Besides that, for each major, it can be subdivided into certain categories based on the blast loading produced on the structure or acting on the structure.

Table 2.2 Categories of Blast Load

Charge Confinement	Categories
Unconfined	Explosion in the air
	The explosion near the ground
Confined	Fully ventilation
	Partially Confined
	Fully Confined

Source: Draganic and Sigmund (2012)

The free air blast pressure or open-air explosion occurs between the explosive charge and the structure it spreads without amplifying the initial shock wave for the unconfined charge. According to Draganic et al. (2012), These explosions are located at a given distance and height away from the structure and a wave increase occurs due to ground reflection before contact with the structure and the height limitations of these explosions are two to three times the height of a single-storey or two-storey structure. Besides that, Mirgal et al. (2014) stated the unconfined explosions can occur as an air-burst or a surface burst. The air burst environment or the air explosion is produced by explosions occurring above the ground surface and at a distance from the building structure so that the initial shock wave, propagating away from the explosion, impinges on the ground surface before the structure arrives. In addition, when the charge is located near or on the ground, the explosion is considered as a surface burst. The ground surface reflects and reinforces the initial wave of the explosion to produce a reflected wave (Olarewaju et al., 2011).

However, for confined load, when the explosion occurs in the structure, the peak pressure associated with the initial wave is very high as the refraction within the structure has been increased. In addition, depending on the degree of containment, high temperatures and the accumulation of gaseous products, chemical reactions in the blast would produce more pressure and increase the duration of the load within the structure (Draganic and Sigmund, 2012). So, due to the increase combined effects of this pressure, it can lead to the human injury.

2.2.2 Propagation of The Blast Wave

There are usually three types of reflection that give a negative effect or impact on a surface, such as normal reflection, oblique reflection, and Mach stem reflection. The simplest type is the normal reflection when the angle of the incident is zero, 0°. The reflected pressure for normal reflection is greater than that for oblique and Mach stem reflections that occur when there is an angle of incident between the shock front and the reflective surface (Peng, 2009). The oblique reflection and the reflection of the Mach stem occur when the angles of the incident are less than 40° and more than 40° respectively.

Thus, blast wave reflection occurs when the incident blast wave strikes a steep surface like open surface with no wall barrier at all or wall front. Figure 2.4 below shows the pattern of the reflected wave in the outward movement of the airborne blast wave. Remennikov (2007) stated that the wave front did not reach the ground at the first stage.

However, the second stage was somewhat later in time, and a reflected wave was produced at the third stage, indicated by the dashed line.

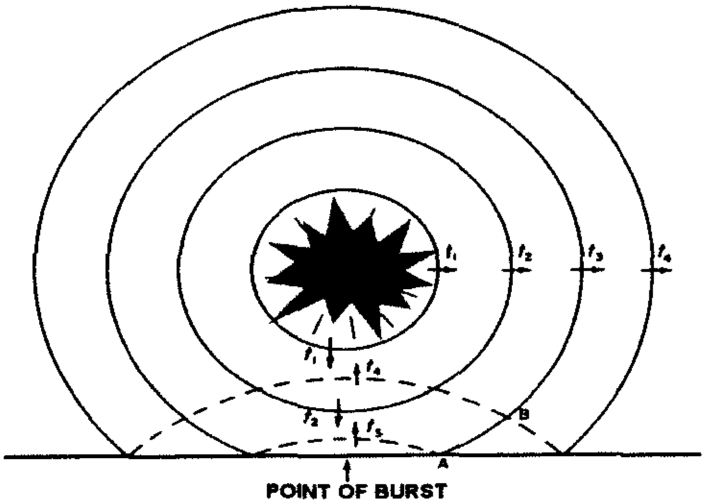

Figure 2.4 Blast wave from a surface burst

Source: Prummer (2007)

2.2.2.1 Without an Obstruction of Wall

In the free-field blast pressure wave, the supersonic detonation forms gasses within a high explosive that experience intense expansion that compresses the surrounding air layer and forms a blast wave. Therefore, in a high-pressure wave front, the blast wave will expand from the explosive charge. This blast wave propagates along the surface in a free-field application until it is no longer supersonic (Rouse, 2010). Otherwise, it will result in injuries and fatality if the human responds directly to the blast.

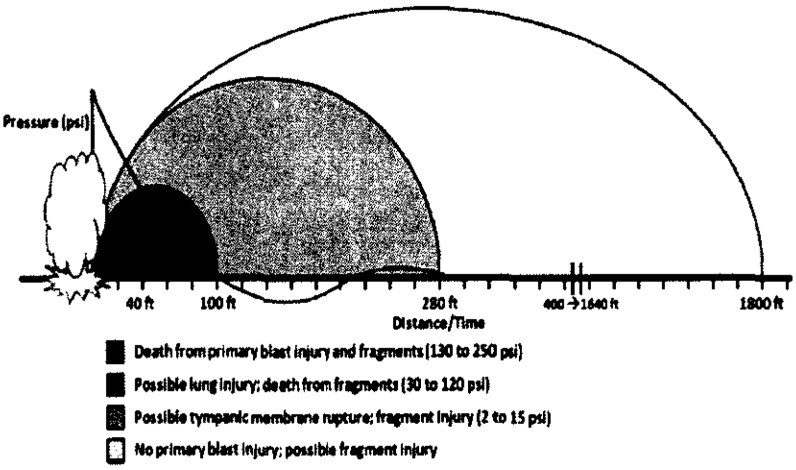

Figure 2.5 Illustration of Friedlander curve with maximum effective radius of primary and secondary blast injuries of an open spaced without any barrier wall, 155 mm mortar shell explosion with 200 lbs (100 kg) of TNT equivalent

Source: Kang et al. (2012).

Kang et al.(2012) reported that the almost instantaneous peak in ambient air pressure declines rapidly in the open space environment as it travels away from the explosion epicenter through a well-defined pressure against time curve called the "Friedland wave" whereas when in an enclosed space, this typical relationship does not occur, as blast waves deflect, reflect, and coalesce, which can magnify the destructive power eight to nine times and cause significantly greater injury.

In addition, the distance from the blast event is one of the important factors affecting the magnitude of the blast overpressure. The closer the object to an explosion, the greater the blast overpressure. Hunt (2013) states that the peak overpressure will decrease to one-eighth of the original value if the distance from the explosion is doubled. He also showed that 1 kg of explosive at the center of the detonation could cause the blast overpressure to exceed 500 kPa. So, there may be no worst injury if the object is 3 m from the point of detonation because the blast overpressure could be as low as 20 kPa.

Based on the book of Evaluation of the Effects and Consequences of Major Accidents in Industrial Plants (Casal, 2017), the overpressure, P depends on the position of the human body show in Figure 2.6. If body position is such that no obstruction of the incident wave, P equals the side-on overpressure P, of the blast wave as in Figure 2.6 (a). If the body is upright Figure 2.6 (b), the incident wave is disturbed. Because in relation to the length of the blast wave, the human body is small, the phase of reflection can be neglected. Then the resulting overpressure on the chest wall equals the side-on overpressure P, plus the pressure Q caused by the explosion wind multiplied with the drag coefficient C, of the body:

$$Q = \frac{5P_s^2}{2P_s^2+14\times10^5} \tag{3}$$

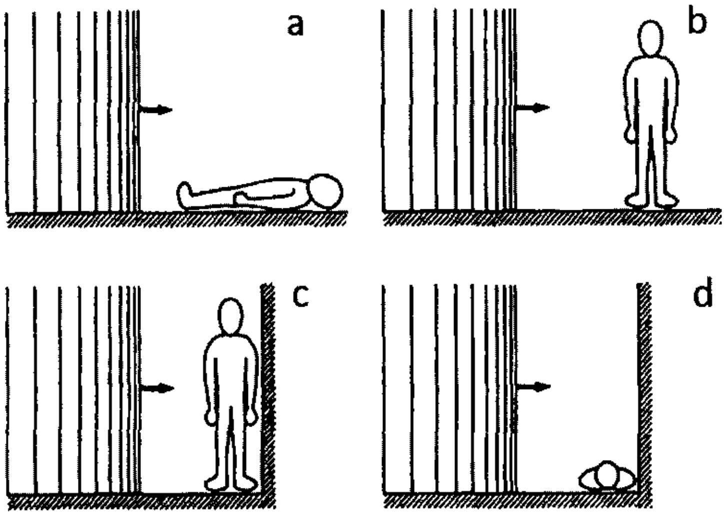

Figure 2.6 Position of human body. (a)No obstruction of incident wave: $P=P_s$. (b)Diffraction of incident wave: $P=P_s+Q$. (c)Body subjected to reflection (standing): $P=P_r$, (d) Body subjected to reflection (prone): $P=P_r$

Source: Casal (2017)

In general, the drag coefficient depends on the structure's shape. If the body is close to a surface that the blast wave can reflect as shown in Figure 2.6(c) and Figure 2.6(d), the pressure P acting on the body equals the reflected pressure P_r:

$$P_r = 2P_s + \frac{(\gamma-1)P_s^2}{(\gamma-1)P_s+2p_0} \tag{4}$$

Figure 2.7 shows the relationship between stand-off distance and net explosive weight which the blast pressure is measure in Pound per square inch. (Brown and Lowe, 2003). It also states that a proven approach to reducing the threat and impact of an explosive blast is to create a stand-off distance between the protected asset and the area where blast could be placed.

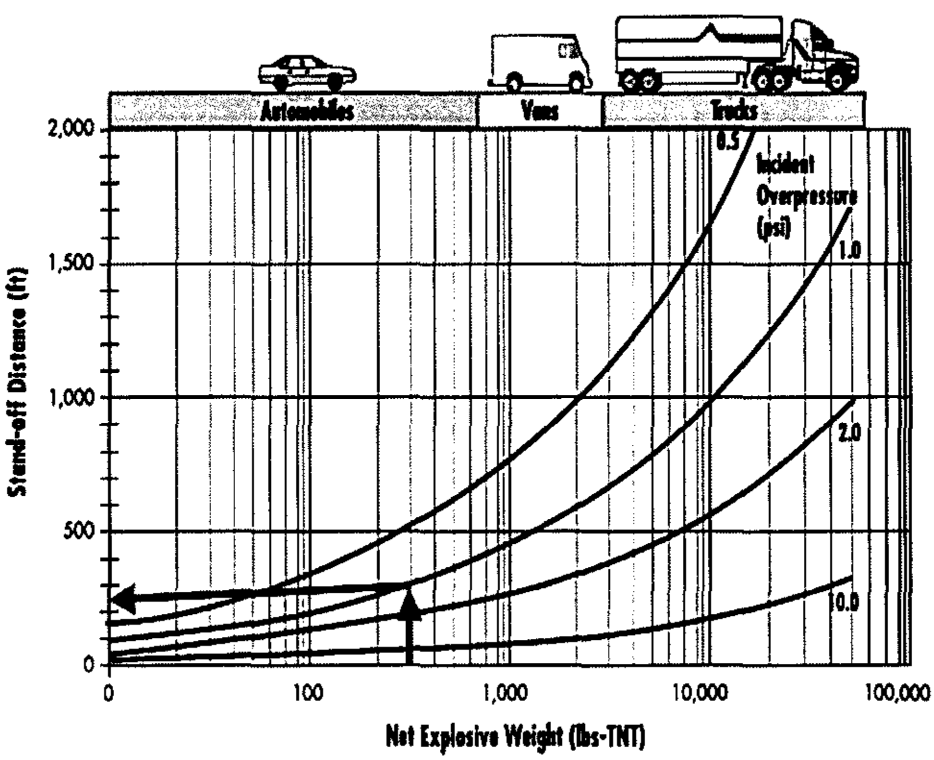

Figure 2.7 Chart of blast pressure against stand-off distance

Source: Brown and Lowe (2003)

Other than that, a source from 'Improvised Explosive Device (IED) Safe Standoff Distance Cheat Sheet Threat' stated two categories of blast which are High Explosives: TNT equivalent ,and Liquified Petroleum Gas such as LPG-Butane or Propane. Whereas in table 2.3, it is shown that every different types of blast will have different explosive mass which in result gives different evacuation distance and safe distance; that is stand-off distances.

Table 2.3 Improvised Explosive Device (IED) safe stand-off distance

	Threat Description		Explosives Mass[1] (TNT equivalent)	Building Evacuation Distance[2]	Outdoor Evacuation Distance[3]
High Explosives (TNT Equivalent)		Pipe Bomb	5 lbs 2.3 kg	70 ft 21 m	850 ft 259 m
		Suicide Belt	10 lbs 4.5 kg	90 ft 27 m	1,080 ft 330 m
		Suicide Vest	20 lbs 9 kg	110 ft 34 m	1,360 ft 415 m
		Briefcase/Suitcase Bomb	50 lbs 23 kg	150 ft 46 m	1,850 ft 564 m
		Compact Sedan	500 lbs 227 kg	320 ft 98 m	1,500 ft 457 m
		Sedan	1,000 lbs 454 kg	400 ft 122 m	1,750 ft 534 m
		Passenger/Cargo Van	4,000 lbs 1,814 kg	640 ft 195 m	2,750 ft 838 m
		Small Moving Van/ Delivery Truck	10,000 lbs 4,536 kg	860 ft 263 m	3,750 ft 1,143 m
		Moving Van/Water Truck	30,000 lbs 13,608 kg	1,240 ft 375 m	6,500 ft 1,982 m
		Semitrailer	60,000 lbs 27,216 kg	1,570 ft 475 m	7,000 ft 2,134 m
	Threat Description		LPG Mass/Volume[1]	Fireball Diameter[4]	Safe Distance[5]
Liquefied Petroleum Gas (LPG - Butane or Propane)		Small LPG Tank	20 lbs/5 gal 9 kg/19 l	40 ft 12 m	160 ft 48 m
		Large LPG Tank	100 lbs/25 gal 45 kg/95 l	69 ft 21 m	276 ft 84 m
		Commercial/Residential LPG Tank	2,000 lbs/500 gal 907 kg/1,893 l	184 ft 56 m	736 ft 224 m
		Small LPG Truck	8,000 lbs/2,000 gal 3,630 kg/7,570 l	292 ft 89 m	1,168 ft 356 m
		Semitanker LPG	40,000 lbs/10,000 gal 18,144 kg/37,850 l	499 ft 152 m	1,996 ft 608 m

Source: Brown and Lowe (2003)

Every meter of stand-off counts in mitigating the effects of a blast. Defining safe stand-off distances can pose major challenges for people who own and operate crowded places, especially when unhindered access to large open spaces is a common feature of such places. Guidance on minimum and maximum safe evacuation distances relative to the size of potential explosive devices as outlined in table 2.4 is available.

Table 2.4 Bomb threat evacuation and its recommended distances

Threat/Description	Explosive Quantity (kg)	Min (m)	Max(m)
Pipe Bomb Small	100	80	575
Pipe Bomb Medium	500	100	860
Pipe Bomb Large	2.5	130	1135
Briefcase	23	185	1520
Compact Sedan	230	270	1915
Cargo Van	1800	375	2410
Small Moving Van	4540	440	3280
Large Moving Van	13600	525	4730

Source: Brown and Lowe (2003)

2.2.2.2 With an Obstruction of Wall

In the previous sub-topic, the interaction of the blast wave in open space was discussed, but when the structure is introduced such as the barrier wall, the blast wave will change that way. Rouse (2010) discussed that providing a blast barrier at the blast parameter event is the way to enhance the survival of blast load structures. This is because when a blast wave charge affects the barrier wall, the blast wave diffracts and reflects around the barrier wall or above it as shown in Figure 2.8. This is because most of the blast wave is not absorbed or transmitted across the barrier, but is reflected around it. The existence of this barrier thus reflects some part of the blast wave from the way it came and wraps around the top of the barrier (Hunt, 2013). The area where the wall affects the blast pressure and causes the pressure to decrease defines the effectiveness of the barrier wall to decrease pressure.

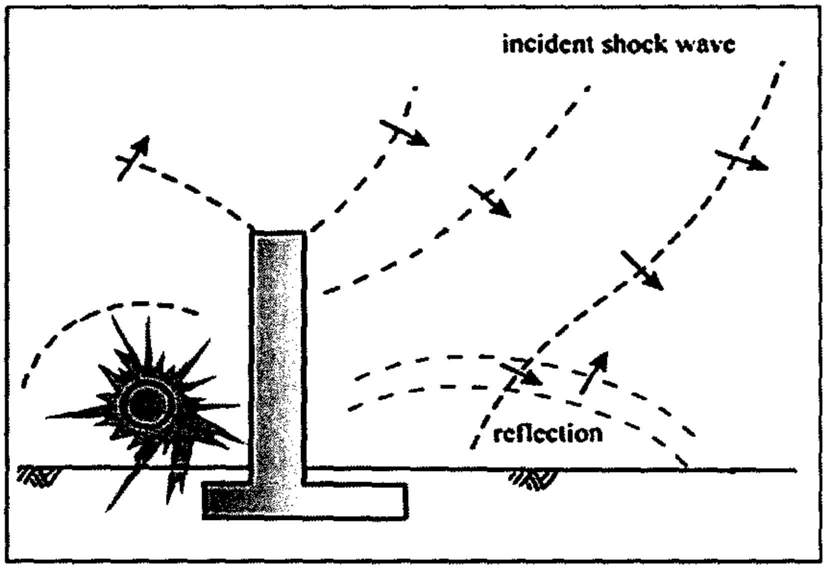

Figure 2.8 Blast wave diffraction over a barrier wall.

Source: Baumgart (2014)

According to Rouse (2010), the existing wall has more effect on the blast pressure affecting the wall-side area than on the wall-free areas. The area was greatly influenced by changes in the height of the wall, while changes in the charge's standoff distance had relatively little influence on the area. Rouse thesis project has the pressure wave which is formed by a hemispherical charge on the table surface. The shock front that the charge produces travels along the surface of contact and expands outward from the charge into the atmosphere.

In addition, experimental results and numerical simulations have been demonstrated as the barrier is one of the effective ways of reducing blast load. So, in propagating the blast wave to the object, it acts as an obstacle. Therefore, some portion of the explosive energy is reflected back, and then the distribution of the blast pressure on the structure behind the barrier is changed and the peak pressure is reduced. When the pressure is reduced, it will provide a standoff distance that can protect human against extreme external explosion and can reduce the fatality rate. One of the suggestions or the best way to protect any object close to the blast event that is by increasing the distance to the standoff. The paper also stated that providing a wall barrier at that perimeter is the simplest way to enhance the survival of human against the blast loads. This is because it can act as a barrier to the propagation of the blast wave (Zhou and Hao, 2008).

2.2.3 Blast Impact on Human

According to (Nguyen et al., 2019), blast injuries are categorized mainly on the basis of how the physical aspects of the explosion act when the injury is caused. The primary blast effects are associated with the blast wave that causes the most vulnerable to injury to organs with high air content such as the lung, intestine, and middle ear. Secondary blast effects are caused by highly energized objects, such as portions of the device enclosure, deliberately added fragments or debris from the vicinity of the device, which are carried by the blast wave and can reach the human body at very high speeds, resulting in soft and skeletal tissue injuries. Tertiary blast effects describe the blunt impact and crush injuries caused by blast-induced personnel or hard objects displacement. Quaternary blast injuries are associated with burns, toxic gas inhalation, or contamination of the environment, and quinary blast injuries may be due to hyperinflammatory behaviours due to toxins added to the explosive as unconventional contents.

Kirkman et al. (2011) also states about the category of blast injury where the tolerance of human blasting is relatively high. However, significant factors determine the severity of the injuries. It also state that blast injuries can be categorised into four classes, (1) Primary Effects; The direct impact on humans due to an explosion is the sudden increase in pressure caused by the blast wave; (2) Secondary Effects; Impact in the case the individual is not supported and can be thrown off-balance, Human tolerance to fragment impact is very low, The injuries from the collapse of a building, and Thermal Injuries; (3)Tertiary Effect; the acceleration of the whole body or parts of the body by the blast wave traumatic amputation of body parts and stripping of tissue; and (4) Quaternary Effects; a further group of miscellaneous injuries includes flash burns caused by the radiant and convective heat of the explosion.

Besides, the classification of blast injury on human is also stated in the book of 'GULF WAR AND HEALTH' by National Academy of Sciences (2014) where it also stated at mostly similar information on the category of blast injury on human. It stated that explosions may cause five major patterns of injury which is primary, secondary, tertiary, quaternary, and quinary. Primary blast injury is caused by the blast wave itself. Followed by the secondary injury is caused by fragments of debris propelled by the explosion. Then, tertiary injury is due to the acceleration of the body or part of the body by the blast wave or blast wind. Next is quaternary injuries that is injury including all other injuries directly caused by a blast but not classified by another mechanism which for instance is burns, toxic-substance exposures and psychologic trauma. And lastly, quinary injuries are illnesses or diseases that result from chemical, biologic, or radiologic substances released by a bomb. The illustration of the class of injuries is as shown in Figure 2.9.

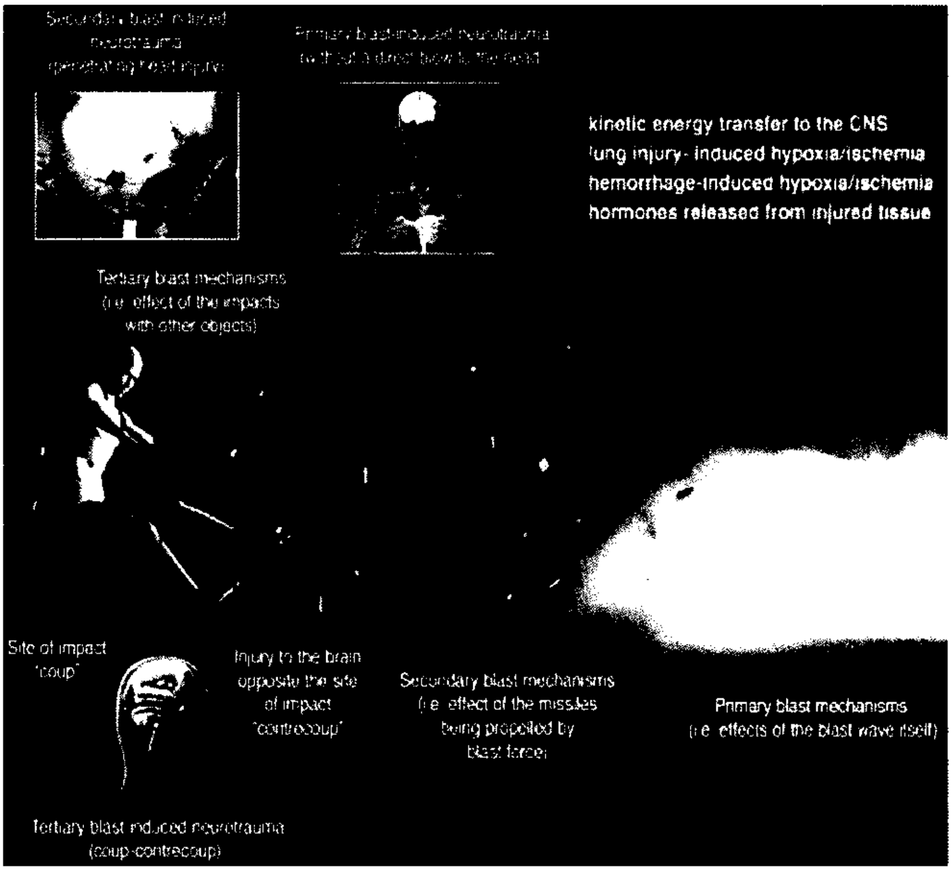

Figure 2.9 Illustration of primary, secondary, and tertiary blast injury

Source: National Academy of Sciences (2014)

Blast injury depends on the pressure level. Likewise, it also depends on the weight of the blast threat itself where the higher the blast pressure, the higher the fatality and casualty potential. Besides that, human body positions and location measures referring to the prevention of unscreened and potentially threatening, also known as stand-off distance, are also factors that may cause fatalities and injuries. The book also has also provided the information from the journal of the Royal Army Medical Corps, Hunterian lecture 1980 which stated about the overpressure effects on surrounding materials and unprotected persons as shown in table 2.5 below.

Table 2.5 Blast pressure effect on unprotected human

Pressure, kPa (Psi)	Effect on Human Body
34.37 (5)	Slight chance of eardrum rupture
103.42 (15)	50% chance of eardrum rupture
206.84 – 275.79 (30 - 40)	Slight chance of severe lung damage
551.58 (80)	50% chance of severe lung damage
689.48 (100)	Slight chance of fatality
896.32–1,241.06 (130 – 180)	50% chance of fatality
1,378.95–1,723.69 (200–250)	100% fatality

Source: National Academy of Sciences (2014)

Besides that, Malhotra et al. (2017) did a research on blast pressure test affecting human and its surrounding causing severe injuries and possible fatalities. According to this paper, the ear is very sensitive to air pressure and responds to even very small variations in air pressure. The ear drum rupture threshold is 34 kPa, but there may be temporary hearing loss at lower levels. Table 2.6 presents basic ear damage information.

Table 2.6 Human ear damage due to blast pressure.

Maximum Effective Overpressure (kPa); it is the highest of incident pressure, incident pressure plus dynamic pressure, or reflected pressure	Type of Damage
35	Threshold of eardrum rupture
325 and above	50 % ruptured eardrums

Source: Malhotra et al. (2017)

As the external blast pressure on the chest wall becomes larger than the internal pressure, the chest wall moves inwards causing injury. The air-containing lung tissues release air bubbles from disrupted lung alveoli into the vascular system, causing the majority of deaths. Table 2.7 provides basic information on damage to the lungs.

Table 2.7 Human lung damage due to blast pressure.

Maximum Effective Overpressure (kPa)	**Type of Damage**
210 to 280	Threshold
560 and above	50 % damaged lungs
700 to 850	Threshold of fatality
900 to 1300	50 % fatality
1400 and above	Near 100 % fatality

Source:Malhotra et al. (2017)

Likewise, according to an experimental test resulted by R. Karl et al., 2010, it summarises the effects of increasing blast pressure on various structures and the human body as in table 2.8.

Table 2.8 Effect of increasing blast pressure on human

Peak Pressure, kPa (Psi)	**Effect on Human Body**
6.89 (1)	Light injuries from fragments occur
13.78 (2)	People injured by flying glass and debris
20.67 (3)	Serious injuries are common, fatalities may occur
534.45 (5)	Injuries are universal, fatalities are widespread
68.9 (10)	Most people are killed
137.8 (20)	Fatalities approach 100%

Source: R. Karl et al., 2010

2.3 AUTODYN

The AUTODYN software is an integrated explicit analysis tool program specifically designed to model non-linear dynamic issues using finite elements (FE), finite volume (CFD) and mesh-free particles (SPH) to solve non-linear dynamic problems of solids, fluids, gas and their interaction. AUTODYN also offers multi-solver coupling for multi-physics, including FE, CFD and SPH coupling. The material model of AUTODYN is subject to the RC wall, the blast load and the domain of air. For the use of these materials, the effects of strain rate and the appropriate coupling between air-solid interface should be considered.

AUTODYN software was developed to solve non-linear dynamic problems. Differential governing equations are derived from the laws of mass, momentum and energy conservation. These laws are always being fulfilled. Furthermore, for material modelling that links stress to deformation and internal energy, a constitutive law is required. In AUTODYN, this differential equation system is solved by combining finite volume, finite element and mesh-free solver technologies (Ramezani et al., 2018). The methodology is based on explicit time integration. High explosive detonation is carried out so that at the time of the detonation wave the fraction of explosive energy is inserted into the cell. This procedure is intended to thoroughly detonate the high explosive and convert it into explosive products.

Based on the previous research work conducted by Casal (2017), Nystrom and Gylltoft (2009), Kamal and Eltehewy (2012) and Wang et al., (2013), Concrete and steel are assigned to the default material in AUTODYN such as CONC-35MPA and STEEL 4340. The material for concrete and steel is based respectively on the material model of Riedel, Hiermayer and Thoma (RHT) and the material model of Johnson-Cook (JC). However, the Piecewise Johnson-Cook is used to describe the behaviour of steel (Nystrom and Gylltoft, 2009) and the modified parameter RHT is used to describe the behaviour of concrete (Tu and Lu, 2009) to provide accurate approximation by parameter in each of the research works carried out.

2.3.1 Material Model for Concrete

A proper model that reflects concrete material behaviour at a high strain rate is vital to obtain a reliable prediction of concrete behaviour under blast loads. The material model developed by Riedel, Hiermayer and Thoma (RHT) is adopted in this study (Riedel et al., 1999). The RHT concrete model for brittle materials is an advanced plasticity model. Modelling concrete dynamic loading is particularly useful. The model includes pressure hardening, strain hardening, strain hardening, third invariant meridian compressive and tensile dependency as well as strain softening damage model. This model also uses the p–α state equation (Herrman, 1969) to represent the thermodynamic behaviour of concrete at high stress, providing a reasonably detailed description of compaction behaviour at low stress ranges. It is established that at the same pressure and temperature the specific internal energy for the porous material is the same as the solid material. The model consists of three pressure-dependent surfaces, a fracture surface, an elastic limit surface, and the crushed material's residual strength surface. Figure 2.10 shows these strength surfaces.

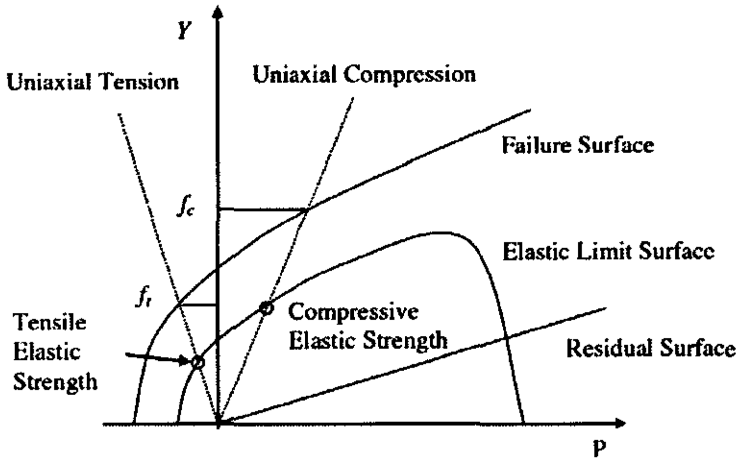

Figure 2.10 Maximum strength, yield strength and residual strength surfaces.

Source: ANSYS (2018)

The failure surface, Y_{fail} is defined as a function of the normalised pressure, lode angle and strain rate:

$$Y_{fail}(p^*, \theta, \varepsilon) = Y_c(p^*).r_3.F_{rate}(\varepsilon) \qquad (5)$$

where $Y_c(p^*)$ is the comprehensive meridian and it represents by

$$Y_c(p^*) = f_c[A.\left(p^* - p^*_{spall}F_{rate}(\varepsilon)\right)^N] \qquad (6)$$

where, f_c denotes the material uniaxial compressive strength, A is failure surface constant, N is failure surface exponent, $p^* = p/f_c$ is normalised pressure; and $p^*_{spall} = f_t / f_c$, where f_t is the material uniaxial tensile strength; F_{rate} (ε) represents the dynamic increase factor (DIF) as a function of the load rate, ε. $r_3(\Theta)$ defines the model's third invariant dependence as a function of the second and third load invariant and a strength ratio at zero load Q_2. Figure 2.11 illustrates the tensile and comprehensive meridian on the stress π plane.

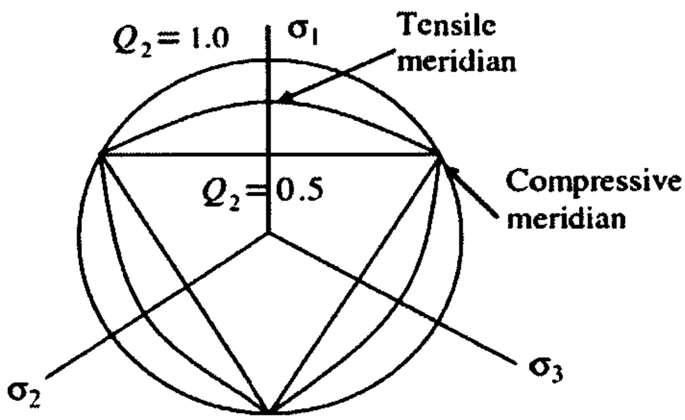

Figure 2.11 Third invariant depend on stress π plane.

Source : ANSYS (2018)

The elastic limit surface is scaled from the failure surface,

$$Y_{elastic} = Y_{fail} \cdot F_{elastic} \cdot F_{cap}(p) \tag{7}$$

where $F_{elastic}$ is the ratio of the elastic strength to failure surface strength. $F_{cap}(p)$ is a function that limits the elastic deviatoric stresses under hydrostatic compression, varying within the range of (0,1) for pressure between initial compaction and solid compaction pressure.

The residual failure surface is defined as

$$Y^*_{residual} = B \,.\, (p^*)^M \tag{8}$$

where B is the residual failure surface constant, and M is residual failure surface exponent.

After the hardening phase, additional material plastic strain results in reduced damage and resistance. Damage from the relationship is assumed to accumulate:

$$D = \Sigma \frac{\Delta \varepsilon p}{failure_{\varepsilon p}} = \Sigma \frac{\Delta \varepsilon p}{D_1 \left(p^* - P^*_{spall}\right)^{D_2}} \tag{9}$$

where D_1 and D_2 are material constants for effective strain to fracture.

The damage accumulation can have two effects in the model, reduction in strength and reduction in shear stiffness as below

$$Y^*_{fracture} = (1 - D)Y^*_{failure} + DY^*_{residual} \quad (10)$$

$$G_{fracture} = (1 - D)G_{elastic} + DG_{residual} \quad (11)$$

where $G_{elastic}$, $G_{residual}$ and $G_{fracture}$ are the shear modulus.

To simulate the beam response, it was necessary to make some modification of the model. The work concluded that in the case of blast loading, the main-stress tensile-failure mode was needed to describe the structure behaviour rather than the hydrodynamic tensile-failure model used as the default. The change to principal stress tensile-failure model leads to a cut-off the strain rate dependence of the ultimate tensile strength. In addition, Nystrom and Gylltoft (2009) performed the same modification in the numerical study of reinforced concrete wall subjected to blast loading and fragment loading to get the accurate result.

2.3.2 Material Model for Steel Reinforcement

A Johnson-Cook (JC) material model (Johnson and Cook, 1983) was used to describe the steel reinforcement behaviour. This model represents the strength behaviour of material subject to high strain, high strain rates, and typically metal high temperature. The model defines the yield stress Y as

$$Y = \left[A + B\varepsilon_p^n\right]\left[1 + c\ln\frac{\varepsilon_p}{\varepsilon_0}\right]\left[1 - T_H^m\right] \quad (12)$$

where ε_p is effective plastic strain; $\varepsilon_p = \varepsilon / \varepsilon_0$ is normalised effective plastic strain rate for $\varepsilon_0 = 1 s^{-1}$; homologous temperature, $T_H = (T-T_{room}) / (T_{melt} - T_{room})$ where T_{room} is room temperature and T_{melt} is melting temperature; and A, B, C, n and m are five material constants. The first, second and third brackets in the above equation, respectively, represent stress as a function of strain, strain rate effect on yield strength and thermal softening. The constant A is the basic yield stress at low stress, while the effect of strain hardening is represented by B and n. Besides the JC material model, Nystrom and Gylltoft (2009) is used piecewise linear Johnson-Cook material model including strain hardening but not strain-rate and thermal effects to conduct numerical studies on blast pressure of with and RC wall as a barrier.

2.3.3 Material Model for Air and High Explosive

The numerical approach to the analysis of the air-structure interface is the Arbitrary Lagrange Euler (ALE). This approach allows the use of Lagrange and Euler approaches to simultaneously model different parts of the solvers such as structure, fluids and gases. These different solvers are then coupled together in space and time.
Air is modelled in the numerical model by an ideal state gas expression (EOS), which is one of EOS's simplest forms. The pressure is related to energy is given by

$$p = (\gamma - 1)\rho e \tag{13}$$

where γ is a ratio of specific heat and ρ is air density, e is the specific internal energy, with the gamma law EOS under standard atmosphere pressure and γ =1.4, its initial energy is e=2.068 x 10^5 kJ/kg.

TNT the high explosives are typically modelled by using the Jones-Wilkins-Lee (JWL) EOS, which model the pressure generated by chemical energy and can be represent as follows:

$$P = A\left(1 - \frac{\omega}{R_1 V}\right)e^{-R^1 V} + B\left(1 - \frac{\omega}{R_2 V}\right)e^{-R_2 V} + \frac{\omega E}{V} \tag{14}$$

where P is the detonation of high explosive, V is the specific volume, and E is specific internal energy, and A, B, R_1, R_2 and ω are material constant. The TNT explosive charge, A, B, R_1, R_2, and ω are 3.7377 × 10^5 MPa, 3.747 × 10^3 MPa, 4.15, 0.9 and 0.35, respectively which have been determined from dynamic experiments.

AUTODYN tends to cover a wide range of dynamic applications due to its ability to integrate Lagrangian and Eulerian techniques. The Eulerian representation solver allows materials to flow from cell to cell while the structured mesh number I, J, K is fixed in space. Euler uses the upwind differential scheme for the first order to solve the equation of continuity. Implementation in a cell allows multiple materials.

2.4 Summary

This chapter discusses several studies on human blast pressure with and without a wall as a barrier. There is limited publication on the RC wall as a barrier from blast pressure based on the experimental works reviewed. The work carried out so far is limited on the experimental work for the performance of steel reinforcement used in the RC wall subjected to blast load (Yan et al., 2011). Commercial 3D FE numerical simulation package such as AUTODYN and LS-DYNA are developed and validated in the numerical studies associated with blast load to understand the behaviour of blast pressure. Usually, the parametric study is considered especially on the effects of load weight, standoff distance, and obstacles are present during blast propagation which in the present study is RC wall as a barrier. In addition, as according to Rouse (2010), the main importance of blast barrier walls for the RC wall as a barrier is the reduction of casualty rates due to the standoff distance and the impact of the barrier wall on blast pressure. Depending on the documentation, the levels of pressure associated with certain critical organ failures in humans vary. Therefore, there is a wide variability in the pressure levels cited and their relationship to the human body reaction. However, this concept is still to be studied through numerical analysis in the case of blast pressure with and without wall. Accordingly, the present work considers the numerical modelling of 30 lbs TNT blast and numerical analysis of blast parameters with and without wall as a barrier to be investigated before the effect of blast pressure on humans is relatively assessed.

CHAPTER 3

METHODOLOGY

3.1 Introduction

This chapter describes the current research methodology. First, by using ALE in the AUTODYN 3D non-linear FE software package, it presents the blast pressure 3D model. Then followed by the numerical approach via AUTODYN to assess different parameters of the blast pressure at different conditions. By using this platform, the blast will be modelled and then remap into the air volume at different condition according to the cases involved in this study. This study will investigate the blast pressure in three conditions which; blast without wall as case 1, blast with wall as a barrier as case 2, and blast effect on the human. Thus, this chapter also explains about the detail of the RC wall model and its setup used, and the study on the relationship of blast load pressure and its impact on human whether it caused casualty and fatality or not. In the last part of this chapter, it summarises the methodology flow. The present research methodology of numerical analysis procedure can be translated into the flowchart as explained in Figure 3.1 below.

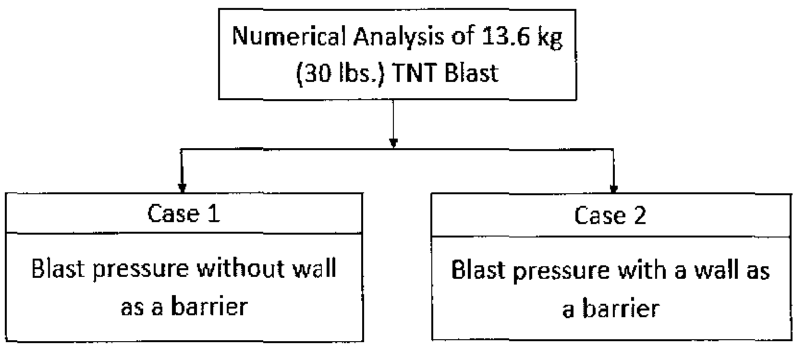

Figure 3.1 Methodology Flow Chart

3.2 Numerical Modelling in AUTODYN

In this study, AUTODYN used for numerical analysis makes it possible to evaluate blast overpressure and its impact on the structure in this study. The ALE solver, as shown in Figure 3.2, is used as a mesh-based hybrid between the Lagrangian and Eulerian method. This present study has implemented the Euler solvers. The Euler solver used are also is in AUTODYN-2D and 3D.

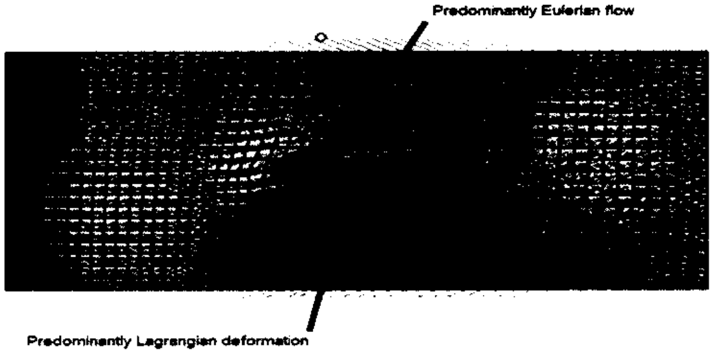

Figure 3.2 ALE solver technique in AUTODYN

Source: ANSYS AUTODYN (2011)

The identification of the solid elements used is performed in ANSYS-Workbench before the RC wall can be exported to AUTODYN solver for blast and impact analysis. The line body is used and treated as a perfect bond between steel reinforcement and concrete in the analysis for the steel reinforcement in the concrete. The eight nodes hexahedral element as shown in Figure 3.3 is used for solid element. This element is suitable for transient dynamic applications including large deformations, large strains, large rotations and complex conditions of contact. Based on Wilkins et al. (1974), the formulation results in an exact calculation of the volume even for distorted elements.

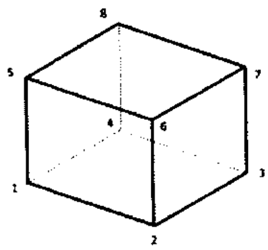

Figure 3.3 Eight nodes hexahedral element.

The standard material model for 35 MPa (CONC-35MPA) concrete in the material library of the AUTODYN is used to describe the concrete behaviour. Some modification is made to the main-stress tensile failure to describe the behavior of the structure in the case of blast loading, instead of the hydrodynamic tensile failure model used as the default in the RHT model, the properties of the material are as shown in table 3.1. On the other hand, the standard model of STEEL-4340 is used in the material library of the AUTODYN to describe the behavior of steel reinforcement. Johnson and Cook (JC) (Johnson and Cook, 1983) developed this material model and is known as the JC model. Table 3.2 shows the material properties respectively. For the preliminary numerical studies based on the RC wall constructed by Yan et al. (2011), the concrete compressive strength and steel yield stress are changed accordingly.

Table 3.1 Employed material data for Concrete input to the RHT

Equation of state	**Linear**
Reference density	2.75000E+00 (g/cm^3)
Porous density	2.31400E+00 (g/cm^3)
Porous sound speed	2.9000E+03 (m/s)
Initial compaction pressure	2.33000E+02 (kPa)
Solid compaction pressure	6.00000E+00 (kPa)
Compaction exponent	3.00000E+00 (none)
Solid EOS	Polynomial
Bulk Modulus	3.52700E+07 (kPa)
Parameter A2	3.95800E+07 (kPa)
Parameter A3	9.04000E+06 (kPa)
Parameter B0	1.22000E+00 (none)
Parameter B1	1.22000E+00 (none)
Parameter T1	3.52700E+02 (kPa)
Parameter T2	0.00000E+00 (kPa)
Reference temperature	3.00000E+02 (K)
Specific heat	6.54000E+02 (J/kgK)
Thermal conductivity	0.00000E+00 (J/mKs)
Compaction Curve	Standard

Table 3.1 Continued

Equation of state	Linear
Strength	**Johnson Cook (JC)**
Shear modulus	1.67000E+07 (kPa)
Compressive Strength (fc)	3.50000E+04 (kPa)
Tensile Strength (ft/fc)	1.00000E-01 (none)
Shear Strength (fs/ft)	1.80000E-01 (none)
Intact Failure Surface Exponent A	1.60000E+00 (none)
Intact Failure Surface Exponent N	6.10000E-01 (none)
Tens./Comp. Meridian Ratio (Q)	6.80500E-01 (none)
Brittle Ductile Transition	1.05000E-02 (none)
G (elas.)/(elas.-plas.)	2.00000E+00 (none)
Elastic Strength / ft	7.00000E-01 (none)
Elastic Strength / fc	5.30000E-01 (none)
Fractured Strength Constant B	1.60000E+00 (none)
Fractured Strength Exponent M	6.10000E-01 (none)
Compressive Strain Rate Exp. Alpha	3.20000E-02 (none)
Tensile Strain Rate Exp. Delta	3.60000E-02 (none)
Max. Fracture Strength Ratio	1.00000E+20 (none)
Use CAP on elastic Surface?	Yes
Failure	**None**
Damage Constant, D1	4.00000E-02 (none)
Damage Constant, D2	1.00000E+00 (none)
Minimum Strain to Failure	1.00000E-02 (none)
Residual Shear Modulus Fraction	1.30000E-01 (none)
Tensile Failure	Hydro (Pmin)
Erosion	**Geometric Strain**
Erosion Strain	2.00000E+00 (none)
Type of Geometric Strain	Instantaneous

Table 3.1 Continued

Equation of state	Linear
Material Cutoffs	-
Maximum Expansion	1.00000E-01 (none)
Minimum Density Factor	1.00000E-04 (none)
Minimum Density Factor (SPH)	2.00000E-01 (none)
Maximum Density Factor (SPH)	3.00000E+00 (none)
Minimum Sound speed	1.00000E-06 (none)
Maximum Sound speed	1.01000E+20 (m/s)
Maximum Temperature	1.01000E+20 (K)

Table 3.2 Employed material data for TNT, input to the JWL EOS

Equation of state	**Linear**
Reference density	7.83000E+00 (g/cm^3)
Bulk Modulus	1.59000E+08 (kPa)
Reference temperature	2.95150E+02 (K)
Specific heat	4.77000E+00 (J/kgK)
Thermal conductivity	0.00000E+00 (J/mKs)
Strength	**Johnson Cook (JC)**
Shear modulus	8.1800E+07 (kPa)
Yield stress	7.2000E+05 (kPa)
Hardening constant	5.10000E+05 (kPa)
Hardening exponent	2.36000E-01 (none)
Thermal softening exponent, m	1.03000E+00 (none)
Melting temperature	1.793000E+03 (none)
Ref. strain-rate (l/s)	1.00000E+00 (none)
Failure	**None**
Erosion	**None**

In this research study, the pressure transducers (gauges) were placed 18 ft away from the centre of the charge weight of 30 lbs TNT charge weight. Validation by the similarities of present study with (Yan et al., 2011) is the result verifying the model of 30 lbs TNT that is remapped into in the following numerical analysis appraisal.

The initial detonation of the propagation of the explosive and blast wave is modelled with a wedge-shaped 2D axial symmetry to model the initial spherical blast for the blast load modelling. As shown in Figure 3.4, the wedge filled with the calculated 13.61 kg load circle equivalent to 30 lbs of the TNT material model and the remaining area outside the circle are filled with the air material model. As shown in Figure 3.5, the detonation starts and runs until the blast wave reaches 1 m from the center of the detonation. The "fill" file consists of the blast overpressure history being created and will be used for additional remapping function in a type of 3D air volume.

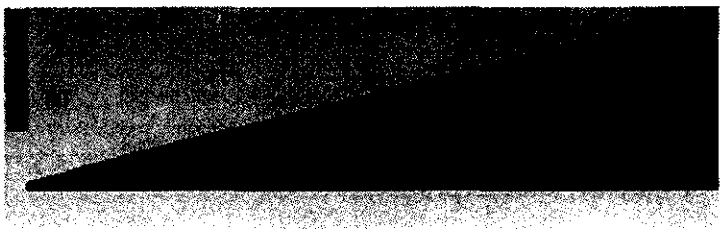

Figure 3.4 The 1 m wedge (2D) filled with TNT and air.

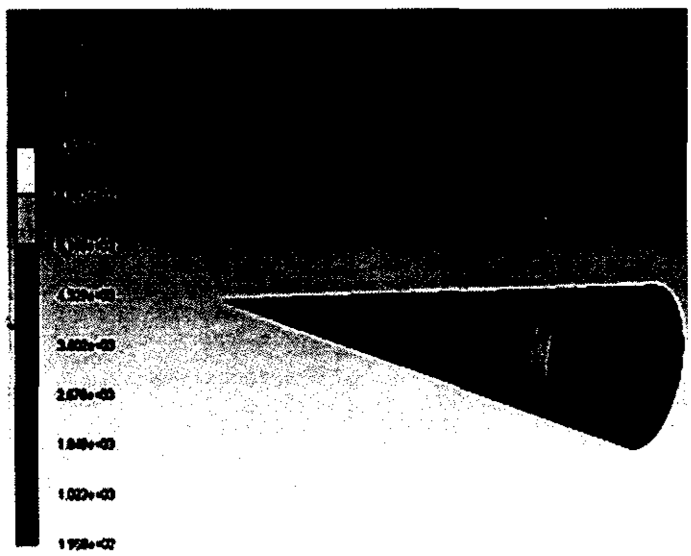

Figure 3.5 Pressure contours in 1 m wedge (3D) during solving progress.

The standard air constant in the material library of the AUTODYN is used to describe the air behaviour being modelled through the ideal state gas expression (EOS). In contrast, the standard TNT model modelled by Jones-Wilkins-Lee EOS is used to describe the behaviour of the explosive. Both material properties are listed in Table 3.3 and Table 3.4, respectively.

Table 3.3 Employed material data for air, input to the ideal gas EOS

Equation of state	**Ideal Gas**
Reference density	1.22500E+00 (kg/m^3)
Specific heat	7.17600E+02 (J/kgC)
Adiabatic exponent γ	1.40000E+00 (none)
Reference temperature	1.50500E+01 (c)
Specific internal energy	2.00000E+05 (J/kg)

Table 3.4 Employed material data for TNT, input to the JWL EOS

Equation of state	**JWL**
Reference density	1.63000E+00 (g/cm^3)
Parameter A	3.73770E+08 (kPa)
Parameter B	3.74710E+06 (kPa)
Parameter R_1	4.15000E+00 (none)
Parameter R_2	9.00000E-01 (none)
Parameter ω	3.50000E-01 (none)
C-J Detonation velocity	6.93000E+03 (m/s)
C-J Energy / unit volume	6.00000E+00 (kJ/m^3)
C-J Pressure	2.10000E+00 (kPa)
Strength	**None**
Failure	**None**
Erosion	**None**

3.2.1 Blast Pressure Analysis

Initially, in the numerical simulation, the air volume type 1 of 2.5 m x 2.0 m x 12.481 m is used to assess the blast overpressure of the calculated explosive which is TNT charge circle in an open space without taking into consideration of the RC wall structure. The air volume type 2 and type 3 has the same size of 12.0 m × 11.0 m × 3.0 m size in (I, J, K) direction is used with grid size on I, J, K direction of 18, 22, 72 respectively. It is to assess the blast pressure of the calculated explosive for both cases of with and without wall as a barrier.

3.2.1.1 Air Volume Type 1

Figure 3.6 shows the air volume with pressure gauge where pressure is determined at 1.219 m (4 ft.) height and 5.486 m (18 ft.) away from the centre of the charge weight respectively. Air flow is allowed at all air volume boundaries. After the 30 lbs TNT is modelled and verified with numerical analysis in air volume type1 with experimental test of Yan et al. (2011), the blast model is remapped into the air volume type 2 and type 3 of each case study.

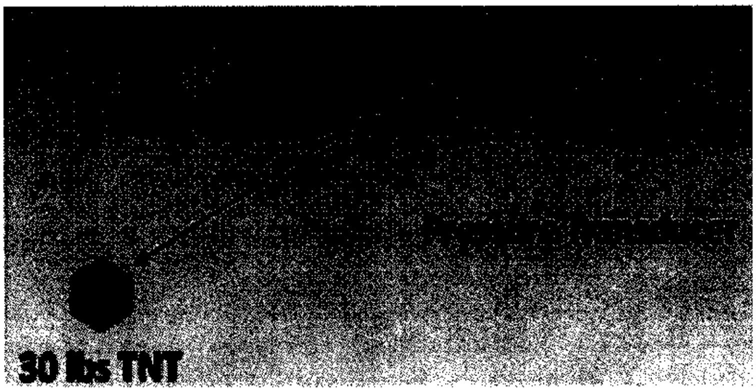

Figure 3.6 blast pressure at 18 ft from centre of charge weight.

3.2.1.2 Air Volume Type 2

Numerical analysis for case 1 is the next stage in the methodology where it is done in a free field explosion without taking into consideration of the RC wall structure model. Figure 3.7 shows the air volume type 2 with pressure gauge for case 1. Case1 and case 2 has the same position of pressure gauge plotted. The pressure gauge plotted with pressure gauge 1 until 6 placed at 4 ft, 8 ft, 12 ft, 16 ft,20 ft, and 24 ft away respectively from the centre of the charge weight.

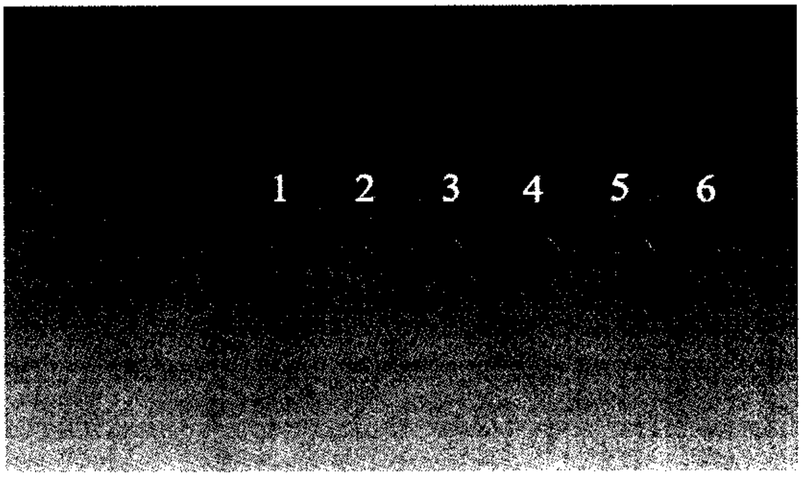

Figure 3.7 Pressure gauge plotted in case 1.

3.2.1.3 Air Volume Type 3

Numerical analysis for Case 2 is the next stage in the methodology where it is done in a free field explosion without taking into consideration of the RC wall structure model. Figure 3.8 shows the air volume type 3 with pressure gauge for Case 2. The available concrete and reinforcement steel material model in this software is used in Case 2 because it considers the strain rate effects and the appropriate coupling between air-solid interface. In addition, Figure 3.9 illustrates the blast wave propagation during numerical analysis with 3D model and the remapped blast pressure vectors in the air volume where the air volume considered the RC wall.

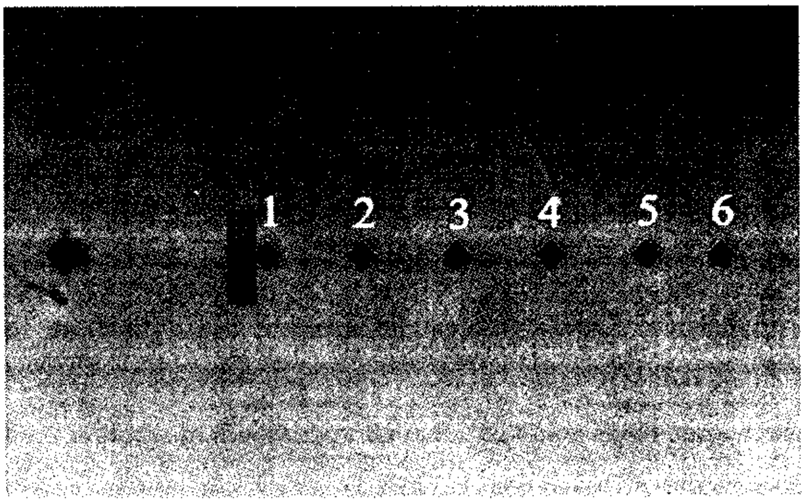

Figure 3.8 Pressure gauges plotted in Case 2.

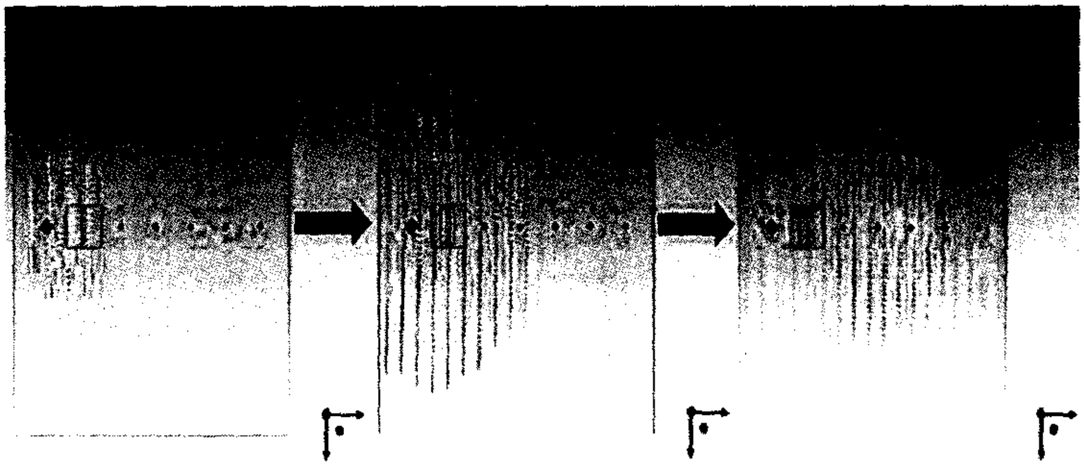

Figure 3.9 Blast simulation flow with RC wall as a barrier.

The result data is presented in a line graph in the numerical analysis to visualise the increasing and decreasing pattern of pressure-time history. The data such as the position (pressure gauge points), value of blast pressure (kPa), and time (msec) is collected. By obtaining the data, the result between cases will be compared and evaluated to identify the blast pressure difference either it is reduced or increased, the percentage difference is calculated by using the following formula:

$$|V1 - V2|[(V1 + V2)^2] \times 100 \quad (6)$$

Finally, in the result and discussion section, a justification on blast parameters effect on human by referring to the literature reviews is conduct to validate the predictions as in Chapter 2. The comparison comprises on the sources of facts and previous studies mainly from journal, news, website, and books related to blast pressure behaviour. The goal of this stage of methodology is to determine the impact of blast pressure at a specific parameter whether it affects human body on casualty and fatality.

3.3 Summary

All of the study's procedure or methodology was explained in this chapter. Research methodology began with the review of literature in which the data serves as a benchmark for this study. In this study, data required for research purposes are numerical results from the simulation of ANSYS AUTODYN and based on references from articles, websites, journals and news for further evaluation.

CHAPTER 4

RESULTS AND DISCUSSION

4.1 Introduction

This chapter is presenting a result for overall numerical simulation done in this study. The main aim of this research is to investigate the blast pressure of 30 lbs TNT on a wall and its surroundings and to study the effect on the blast pressure subjected as a barrier to humans with and without a wall. The simulation was conducted in accordance with the methods discussed in the methodology and this chapter presents the results and detailed analysis of the data.

4.2 Numerical Analysis of 30 lbs. TNT

In the research, the 30 lbs TNT is modelled by using AUTODYN. Based on the blast load model of 30lbs TNT, the "fill" file is obtained and it is verified by comparing the numerical results to experimental result by Yan et al. (2016) at 18 ft away from the center of the blast. Table 4.1 shows the comparison on the maximum peak of blast pressure of 30lbs TNT in numerically model and experiment blast test as in the literature review and Figure 4.1 is the graph comparison between two results.

Table 4.1 Maximum Peak of Blast Pressure

	Time (msec)	**Pressure (kPa)**
Blast Test (Yan et al., 2011)	4.64	490.01
Numerical Analysis in AUTODYN	4.62	494.46

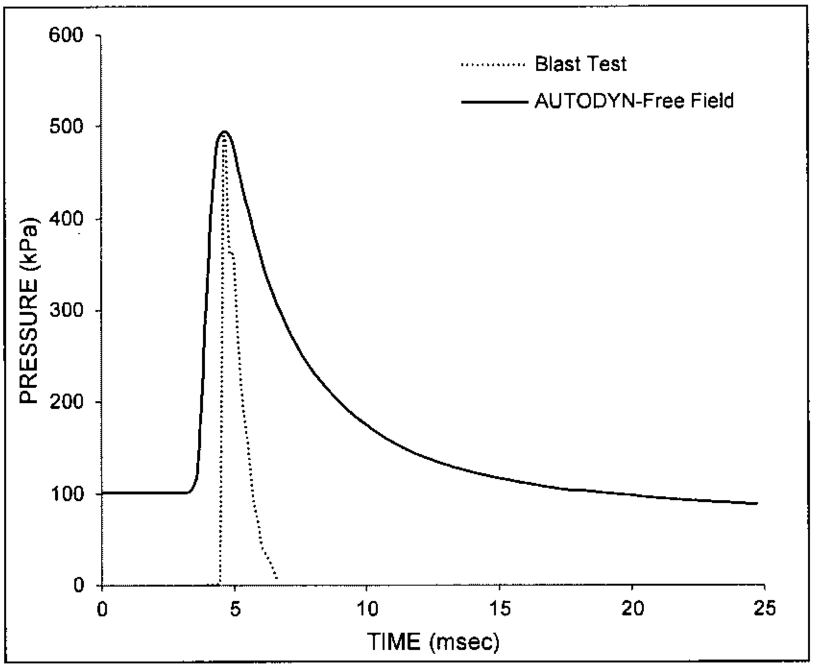

Figure 4.1 Peak blast pressure between numerical simulation and actual blast test.

From the result, it shows that the maximum blast pressure for the distance of 18 ft from the center of blast load is similar for both numerical and experimental analysis which is around 490 kPa. It is verified that the model for 30lbs TNT can be used in the case study of the research which are; case1 blast pressure subjected to human without wall as a barrier, and case 2 blast pressure subjected to human with wall as a barrier.

4.3 Blast Pressure Analysis

4.3.1 Blast Pressure Parameter for Case 1

In the numerical analysis without wall for case 1 which is on blast pressure parameters in open space, the result obtained is as shown in table 4.2 and Figure 4.2.

Table 4.2 Results of peak pressure without RC wall as a barrier

Pressure Gauge	Blast Pressure Without RC wall (kPa)
1	690
2	275
3	180
4	147
5	132
6	125

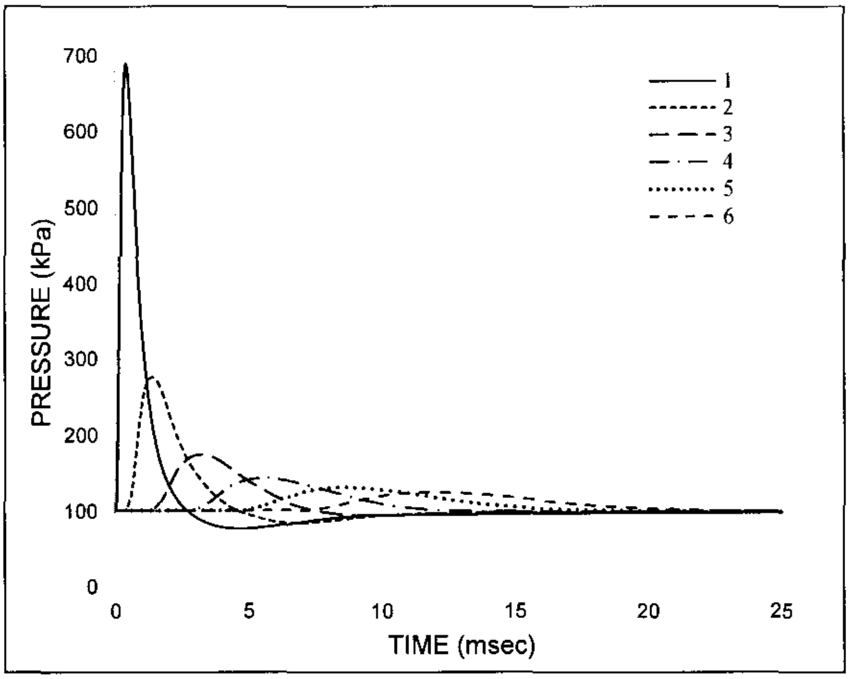

Figure 4.2 Pressure profile without RC wall

For the overall pattern of the graph in Figure 4.2, the result for case 1 shows a decreasing value of blast pressure with increasing value of time and distance.

4.3.2 Blast Pressure Parameter for Case 2

In the numerical analysis for case 2 which is on blast pressure parameters with wall as a barrier, the result obtained is as shown in table 4.3 and Figure 4.3.

Table 4.3 Results of peak pressure with RC wall as a barrier

Pressure Gauge	Blast Pressure with RC wall (kPa)
1	240
2	256
3	175
4	144
5	132
6	125

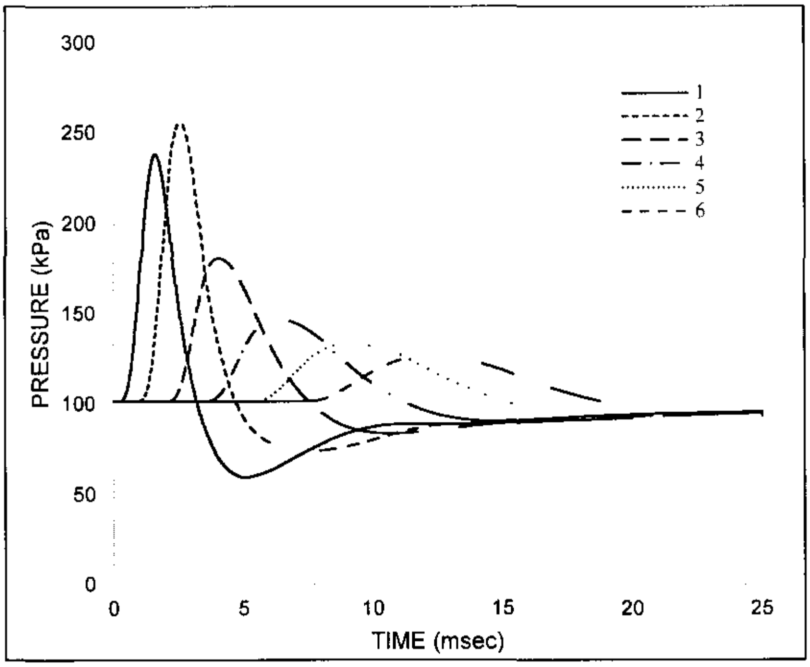

Figure 4.3 Pressure profile with RC wall

Case 2 has resulted in increasing value from pressure gauge 1 to pressure gauge 2. This is due to the presence of wall where the pressure gauge 1 is located behind the wall and it is positioned exactly on the wall surface. Thus, the pressure gauge is completely protected by the wall however it still obtains the impact of blast pressure onto the wall. Nevertheless, for the overall graph pattern, the result for case 2 shows a decreasing value of blast pressure with increasing value of time and distance starting from pressure gauge 2 and above.

To identify the difference between blast pressure before and after a wall is included in the blast event, the numerical analysis results of case 1 and case 2 is compared. The result is compared and percentage difference is obtained as shown in table4.4

Table 4.4 Pressure difference in Case 1 and Case 2

Pressure Gauge	Blast Pressure without RC wall (kPa)	Blast Pressure with RC wall (kPa)	Percentage Difference
1	690	240	65.0
2	275	256	6.90
3	180	175	2.78
4	147	144	2.04
5	132	132	0.00
6	125	125	0.00

The result shows the pressure gauge 1 which is 4 ft from the center of the blast load has the highest pressure reduction value which is 65% reduced after the presence of a wall. The pressure gauge 1 is located exactly behind the wall surface, therefore that area experienced the least pressure due to the protection behind the wall. As expected, the existence of wall can reduce the blast pressure behind it due to the disturbance of shock waves where the RC wall acted as an obstacle to the blast wave propagations. Moreover, the results obtained shows a constant pattern at the end of the pressure gauge modelled which resulted in zero percentage difference. Both result cases also show that they reached the least amount of blast pressure starting from pressure gauge 5 and above.

4.4 Blast Pressure Effect on Human

From the result obtained, the highest peak of blast pressure is 690 kPa without wall and 256 kPa with wall as a barrier. This research will analyse on the impact of blast pressure value obtain in Case 1 and Case 2 based on the literature review as stated in Chapter 2. The effect of blast pressure on human without wall in Case 1 is as shown in table 4.5 and for Case 2 which is blast pressure on human with wall as a barrier is shown in table 4.6.

Table 4.5 Blast pressure effect on human in Case 1

Pressure Gauge	Pressure obtained in Numerical Analysis, kPa	Effect on Human Body		
		(National Academy of Sciences, 2014)	(Malhotra et al, 2017)	(R. Karl et al., 2010)
1	690	Slight chance of death	50% rupture eardrums and 50% damaged lungs	Fatalities approach 100%
2	275	Slight chance of severe lung damage	Possible rupture eardrum and possible damaged lungs	Fatalities approach 100%
3	180	50% chance of eardrum rupture	Possible rupture eardrum and possible damaged lungs	Fatalities approach 100%
4	147	50% chance of eardrum rupture	Possible rupture eardrum and possible damaged lungs	Fatalities approach 100%
5	132	50% chance of eardrum rupture	Possible rupture eardrum and possible damaged lungs	Most people are killed
6	125	50% chance of eardrum rupture	Possible rupture eardrum and possible damaged lungs	Most people are killed

Table 4.6 Blast pressure effect on human in Case 2

Pressure Gauge	Pressure obtained in Numerical Analysis, kPa	Effect on Human Body		
		(National Academy of Sciences, 2014)	(Malhotra et al., 2017)	(R. Karl et al., 2010)
1	240	Slight chance of severe lung damage	Possible rupture eardrum and possible damaged lungs	Fatalities approach 100%
2	256	Slight chance of severe lung damage	Possible rupture eardrum and possible damaged lungs	Fatalities approach 100%
3	175	50% chance of eardrum rupture	Possible rupture eardrum and possible damaged lungs	Fatalities approach 100%
4	144	50% chance of eardrum rupture	Possible rupture eardrum and possible damaged lungs	Fatalities approach 100%
5	132	50% chance of eardrum rupture	Possible rupture eardrum and possible damaged lungs	Most people are killed
6	125	50% chance of eardrum rupture	Possible rupture eardrum and possible damaged lungs	Most people are killed

4.5 Summary

In conclusion, the blast pressure will be reduced when there is a wall as barrier compared to when there is no wall. Besides, the blast pressure behaves in decreasing manner against increasing time and distance and in this research, it is also found that the blast pressure behaves with decreasing value with increasing distance. As in the numerical analysis, it resulted with the highest peak in blast pressure parameter in open space (Case 1) is 690 kPa which the impact on human is prone to possible 100% fatality approach and the injury is from rupture eardrum and damaged lungs. While the minimum peak pressure in Case 1 is 125 kPa which have the effect of possible most people are killed and the possible injury is 50% chance of eardrum rupture and possible damaged lungs. Whereas for the highest peak pressure in Case 2 is 256 kPa which is located at the second pressure gauge. The highest peak in Case 2 has the effects based on literature review concluded as slight chance of severe lung damage, possible rupture eardrum, and approach 100% fatalities. For the minimum peak of 125 kPa in Case 2 is resulted with similar effect to minimum peak pressure in Case 1. Therefore, the overall numerical results show that the pressure obtained is not safe for human, however the presence of wall as a barrier can reduce the amount of blast pressure.

CHAPTER 5

CONCLUSIONS AND RECOMMENDATIONS

5.1 Conclusions

The following conclusions arrived through the numerical and experimental investigation of blast pressure parameters on human with and without wall as a barrier:

1. A 150mm radius charge circle in the numerical modelling is adequate to approximate the recorded blast pressure in the blast test.

2. The blast pressure-time history and its pattern in air volume type 1 is similar to an actual blast test when comparable air grid size with I, J, K (18, 22, 72) is considered. Therefore the 30 lbs TNT blast model is verified and remapped in Case 1 and Case 2.

3. The graph pattern for numerical analysis of Case 1 which consist of air volume type 2 shows a decreasing value of blast pressure with increasing value of time and distance. The peak pressure in Case 1 is 690 kPa which is equivalent to 100% fatality with possible impact of eardrum rupture and lung damage to human. However, at the furthest pressure gauge located resulting in the least blast pressure value is 125 kPa which still gives possible 100% fatality to human with 50% chance of eardrum rupture and 50% chance of lung damage.

4. The graph pattern for numerical analysis of Case 2 which consist of air volume type 3 shows a decreasing value of blast pressure with increasing value of time and distance. The peak pressure in Case 2 is 256 kPa which is prone to most people killed and impact of severe eardrum rupture and lung damage to human. However, at the furthest pressure gauge located resulting in the least blast pressure

value is 125 kPa which is similar to minimum value of peak pressure in Case 1 hence shares the same blast pressure effect on human.

5. Differences between blast pressure resulted in Case 1 and Case 2 shows that the presence of a wall as a barrier can reduce the value of blast pressure at similar condition which is with increasing time and distance.

5.2 Recommendations

In this research, there are several recommendations were identified which needed to be considered for further investigation in order to provide a more reliable data for better development of numerical simulation of blast pressure parameter on human with and without wall as a barrier. This section also includes some suggestion to increase the safety level as well as reducing the blast pressure. The following fields are suggested to expand the present work by:

1. Reducing the blast weight tested so that the blast load used is lower than 30 lbs TNT. This is because it is a better solution for a future research to consider in having a lower blast load due to the 30 lbs TNT used in this study has a very high impact. Thus, this numerical analysis of 30 lbs TNT has not obtained data that is resulted as safe on human although it is located at the farthest point of pressure gauge.

2. Increasing the air domain volume as well as the standoff distance of human from the blast. Since the blast pressure affected by the increasing of distance, the future research should consider to increase the air volume and distance. Then, more pressure gauge can be plotted. Therefore, more data can be obtained and a possible position where human is safe during blast event can be identified.

3. Arrangements of few RC wall as a fence can be consider to reduce more the blast impact on human. For the safety purpose, an implementation of considering RC wall as a fence should be done. It is a practical form of implementation that can be done where several RC wall as a protective barrier from any blast event is applied in real life. This is because through this research, the RC wall has a potential to act as a protection barrier against blast impact.

REFERENCES

ANSYS, 2018. *User's manual* Release 17., ANSYS Inc, Canonsburg, PA.

Baumgart, C.M., 2014. THE EFFECTS OF ADVANCED STRUCTURAL MATERIALS TO By Presented to the Faculty of the Graduate School of the MISSOURI UNIVERSITY OF SCIENCE AND TECHNOLOGY In Partial Fulfillment of the Requirements for the Degree MASTER OF SCIENCE IN Approved by : Jason Bair.

Brown, M.D. and Lowe, A.S., 2003. Explosive blast(FEMA). *Reference Manual to Mitigate Potential Terrorist Attacks Against Buildings*, pp.1–14.

Casal, J., 2017. *Evaluation of the Effects and Consequences of Major Accidents in Industrial Plants.*, Elsevier Science.

DOA., Improvised Explosive Device (IED) Safe Standoff Distance Cheat Sheet Threat. *United States. Department of the Army*. Available at: https://www.hsdl.org/?view&did=440775.

Draganic, H. and Sigmund, V., 2012. Blast Loading on Structures. *Physical Review A*, 93(3), p.10. Available at: https://link.aps.org/doi/10.1103/PhysRevA.93.033817.

Hunt, N.C.A., 2013. Blast injuries. *Essentials of Autopsy Practice: Innovations, Updates and Advances in Practice*, 374(9687), pp.109–133. Available at: http://dx.doi.org/10.1016/S0140-6736(09)60257-9.

Kabu, S., 2015. Blast-associated shock waves result in increased brain vascular leakage and elevated ROS levels in a rat model of traumatic brain injury. *PLoS ONE*, 10(5), pp.1–19.

Kamal, I.M. and Eltehewy, E.M., 2012. Projectile penetration of reinforced concrete blocks: Test and analysis. *Theoretical and Applied Fracture Mechanics*, 60(1), pp.31–37. Available at: https://linkinghub.elsevier.com/retrieve/pii/S0167844212000584 [Accessed: 29 May 2019].

Kang, D.G., Lehman, R.A. and Carragee, E.J., 2012. Wartime spine injuries: Understanding the improvised explosive device and biophysics of blast trauma. *Spine Journal*, 12(9), pp.849–857. Available at: http://dx.doi.org/10.1016/j.spinee.2011.11.014.

Kawi, M.R., 2015. Blast Events. , (April), p. Available at: https://www.bharian.com.my/node/46882.

Kerampran, S., Arrigoni, M. and Locking, P., 2016a. Blast waves propagation and their mitigation. *Greener and safer energetic and ballistic systems*, pp.205–252. Available at: https://hal-ensta-bretagne.archives-ouvertes.fr/hal-01714103.

Kerampran, S., Arrigoni, M. and Locking, P., 2016b. *Blast waves propagation and their mitigation*,

Kirkman, E., Watts, S. and Cooper, G., 2011. Blast injury research models. , pp.144–159.

Malhotra, A., Carson, D. and Mcfadden, S., 2017. ScienceDirect ScienceDirect Blast pressure leakage into buildings and effects on humans. *Procedia Engineering*, 210, pp.386–392. Available at: https://doi.org/10.1016/j.proeng.2017.11.092.

Mamrak, W., Wierszycki, M. and Sielicki, P., 2011. Blast wave propagation in the air and action on rigid obstacles. , p.106.

Mirgal, P., Tikate, P., Suryawanshi, S. and Tande, S.N., 2014. Architectural and Structural Design for Blast Resistant Buildings. *Journal of Civil Engineering and Environmental Technology*, 1(3), pp.103–108. Available at: http://www.krishisanskriti.org/jceet.html.

Nguyen, T.T., Carpanen, A. P., Sory, D., Grigoriadis, D., Newell, G., and Clasper, N. Masouros, S. D., 2019. Experimental platforms to study blast injury. *Journal of the Royal Army Medical Corps*, 165(1), pp.33–37.

Nyström, U. and Gylltoft, K., 2009. Numerical studies of the combined effects of blast and fragment loading. *International Journal of Impact Engineering*, 36(8), pp.995–1005.

Olarewaju, A.J., Kameswara Rao, N.S.V. and Mannan, M.A., 2011. Dimensionless response of underground pipes due to blast loads using finite element method. *Electronic Journal of Geotechnical Engineering*, 16 E(1), pp.563–574.

Peng, W., 2009. Modeling and simulation of interactions between blast waves and structures for blast wave mitigation. -- ... *Mechanical (and Materials) Engineering*, p.102. Available at: http://digitalcommons.unl.edu/cgi/viewcontent.cgi?article=1004&context=mechengdiss.

Prümmer, R., 2007. State of the Art of Explosive Compaction. *Fundamental Issues and Applications of Shock-Wave and High-Strain-Rate Phenomena*, pp.235–244.

R. Karl Zipf, Jr., Ph.D., P.E.K.L.C., 2010. Explosions and Refuge Chambers. Available at: https://www.cdc.gov/niosh/docket/archive/pdfs/NIOSH-125/125-ExplosionsandRefugeChambers.pdf.

Ramezani, A., Hillig, B. and Rothe, H., 2018. A Coupled CFD-FEM Analysis to Simulate Blast Effects on High Security Vehicles Using Modern Hydrocodes A

Coupled CFD-FEM Analysis to Simulate Blast Effects on High Security Vehicles Using Modern Hydrocodes. , (August), pp.74–81.

Remennikov, A., 2007. The state of the art of explosive loads characterisation. , pp.1–25.

Rouse, N. and Consultants, M.W., 2012. The Mitigation Effects of a Barrier Wall on Blast Wave Pressures. *International Society of Explosive Engineers*, pp.1–8.

Rouse, N.T., 2010. The mitigation effects of a barrier wall on blast wave pressures.

Sciences, N.A. of, 2014. *GULF WAR and HEALTH*, United States of America.

Tu, Z. and Lu, Y., 2009. Evaluation of typical concrete material models used in hydrocodes for high dynamic response simulations. *International Journal of Impact Engineering*, 36(1), pp.132–146. Available at: https://linkinghub.elsevier.com/retrieve/pii/S0734743X0800002X [Accessed: 29 May 2019].

Yan, D. et al., 2016. Blast response of full-size concrete walls with chemically reactive enamel (CRE)-coated steel reinforcement. *Journal of Zhejiang University-SCIENCE A*, 17(9), pp.689–701.

Yan, D. et al., 2011. Blast Test of Full-Size Wall Barriers Reinforced with Enamel-Coated Steel Rebar. *Structure Congress 2011, ASCE*, pp.1538–1551.

Zhou, X.Q. and Hao, H., 2008. Prediction of airblast loads on structures behind a protective barrier. *International Journal of Impact Engineering*, 35(5), pp.363–375.